Submitted to Physical Review

RECEIVED
LAWRENCE RADIATION LABORATORY

LBL-226
Preprint c.2

DOCUMENTS SECTION

HIGH-SPIN LEVELS OF ^{92,93,94,95,96}Nb AND ^{94}Tc POPULATED WITH (α, d) AND (α, t) REACTIONS AT 50 MeV

M. S. Zisman and B. G. Harvey

August 1971

AEC Contract No. W-7405-eng-48

LAWRENCE BERKELEY LABORATORY
UNIVERSITY OF CALIFORNIA

TWO-WEEK LOAN COPY

This is a Library Circulating Copy
which may be borrowed for two weeks.
For a personal retention copy, call
Tech. Info. Division, Ext. 5545

LBL-226
c.2

34

DISCLAIMER

This document was prepared as an account of work sponsored by the United States Government. While this document is believed to contain correct information, neither the United States Government nor any agency thereof, nor the Regents of the University of California, nor any of their employees, makes any warranty, express or implied, or assumes any legal responsibility for the accuracy, completeness, or usefulness of any information, apparatus, product, or process disclosed, or represents that its use would not infringe privately owned rights. Reference herein to any specific commercial product, process, or service by its trade name, trademark, manufacturer, or otherwise, does not necessarily constitute or imply its endorsement, recommendation, or favoring by the United States Government or any agency thereof, or the Regents of the University of California. The views and opinions of authors expressed herein do not necessarily state or reflect those of the United States Government or any agency thereof or the Regents of the University of California.

HIGH-SPIN LEVELS OF ^{92,93,94,95,96}Nb AND ^{94}Tc POPULATED WITH (α,d) AND (α,t) REACTIONS AT 50 MeV*

M. S. Zisman and B. G. Harvey

Lawrence Berkeley Laboratory
University of California
Berkeley, California 94720

August 1971

ABSTRACT

The ^{91,92,94}Zr(α,t)^{92,93,95}Nb, ^{90,91,92,94}Zr(α,d)^{92,93,94,96}Nb, and ^{92}Mo(α,d)^{94}Tc reactions have been investigated with a 50 MeV α-particle beam from the Berkeley 88-inch cylotron. High-spin proton excited states observed in the (α,t) reaction, based on comparisons with (^{3}He,d) experiments on the same targets, include: ^{92}Nb (≈ 5 MeV multiplet), ^{93}Nb (1.08, 1.29, ≈ 4.5 MeV), and ^{95}Nb (1.27, 1.65, 2.10 MeV). Two groups of strongly excited states appear in the (α,d) data. Members of the lower group [^{92}Nb(g.s.), ^{94}Nb(0.08 MeV), ^{96}Nb(0.23 MeV)] have been previously identified as being $(\pi g_{9/2}, \nu d_{5/2})_{7^+}$ states. Based on the ^{92}Mo(α,d)^{94}Tc results, the ^{94}Tc ground state can also be assigned 7^+. The higher levels [^{92}Nb(2.58 MeV), ^{94}Nb(2.42 MeV), ^{96}Nb(2.38 MeV), ^{94}Tc(2.68 MeV)] are believed to be either $(\pi g_{9/2}, \nu g_{7/2})_{8^+}$ or $(\pi g_{9/2}, \nu h_{11/2})_{10^-}$ states based on the results of shell model matrix element calculations and the (α,d) structure factors of Glendenning.

I. INTRODUCTION

In recent years there have been many studies of proton configurations in the Zr-Mo region using the (^{3}He,d) reaction.[1-6] Most of this work concentrated on the N = 50 nuclei ^{90}Zr and ^{92}Mo, although (^{3}He,d) data on all of the Zr isotopes was reported in one case.[4] A general feature of these (^{3}He,d) experiments[1-6] is that very few high angular momentum transfers were observed except for the ground states ($g_{9/2}$). The shell-model states expected in this region are $g_{9/2}$, $g_{7/2}$, $d_{5/2}$, $s_{1/2}$, and $h_{11/2}$, which would give rise to both $\ell = 4$ and $\ell = 5$ transitions to various excited states. These high-spin states should be more easily observed with the (α,t) than the (^{3}He,d) reaction because of improved momentum matching for large ℓ transfers in (α,t) [$\vec{Q} \times \vec{R} \approx 6$]. A previous paper on the ^{90}Zr(α,t) and ^{92}Mo(α,t) reactions[7] showed a number of strong levels in the excitation energy region from 4 to 6 MeV in ^{91}Nb and ^{93}Tc which are believed to contain $\ell = 4$ or $\ell = 5$ strength.

Detailed shell-model calculations[8-10] of the spectra of odd mass Nb and Tc isotopes predict the existence of many high-spin levels at low excitation energy. Some of these high-spin levels have been observed in β-decay studies (e.g., ^{91}Mo $\rightarrow$ ^{91}Zr (Ref. 11) and ^{95}Zr $\rightarrow$ ^{95}Nb (Ref. 12)) and Coulomb excitation (e.g., ^{93}Nb(p,p'γ)[13]), but few have been seen in proton transfer reactions[1-6] since they have spins which cannot mix with the available single-proton states in this region. However, some of them are expected[8-10] to be $\frac{9}{2}^+$ and $\frac{7}{2}^+$ and might contain some of the $g_{9/2}$ or $g_{7/2}$ strength and thus be observable in proton stripping.

The (α,d) reaction also shows a preference for populating high-spin final states. This is due, in part, to the same momentum matching effect that occurs for the (α,t) reaction. [$\vec{Q} \times \vec{R} \approx 8$ for the (α,d) reaction in this mass

region.] It is well known, however, that two-nucleon transfer reactions also exhibit a strong selectivity based upon the degree to which the transferred nucleons are correlated in the final state. In the case of the (α,d) reaction, the favored states are those whose wave function can be described by [target core + deuteron]. This structure selectivity has been discussed in detail by Glendenning.[14] In his notation, those states with large "structure amplitudes" will be strongly populated. For the (α,d) reaction the structure amplitudes[14,15] also favor the population of high-spin states. The selectivity of the (α,d) reaction has been used previously[16-21] to locate high-spin levels in the mass region $14 \leqslant A \leqslant 70$. In the Zr-Mo region, the shell model provides many possible high-spin states which might be observed in the (α,d) reaction (e.g., $(\pi g_{9/2}, \nu d_{5/2})_{7^+}$, $(\pi g_{9/2}, \nu g_{7/2})_{8^+}$, $(\pi g_{9/2}, \nu h_{11/2})_{10^-}$, etc.). The high spins of the strongly populated (α,d) states make configuration mixing unlikely, so the wave functions of the levels may be relatively simple. In such a case it may be possible to obtain information on the effective proton-neutron residual interactions which are required for shell-model calculations.

II. EXPERIMENTAL

The experiment was performed with a 50 MeV α-particle beam from the Berkeley 88-inch cyclotron at a beam resolution, ΔE/E, of 0.04%. Target compositions are summarized in Table I. Due to large uncertainties in the target thicknesses, absolute cross sections are accurate only to about ±50%. Relative cross sections, however, should be good to about ±15%. The deuterons and tritons were detected by two counter telescopes, each consisting of a 0.25-mm phosphorus-diffused Si ΔE and 5 mm Si(Li) E detector, and identified with a Goulding-Landis particle identifier.[22]

III. RESULTS

A. $^{92}Zr(\alpha,t)^{93}Nb$

A triton spectrum of the $^{92}Zr(\alpha,t)^{93}Nb$ reaction is shown in Fig. 1. The resolution is 50 keV full width at half maximum (FWHM). As was true for the $^{90}Zr(\alpha,t)^{91}Nb$ reaction,[7] the spectrum is dominated by the $g_{9/2}$ ground state (level 1). (Based on the data of Ref. 7, the unresolved $p_{1/2}$ level at 0.029 MeV is expected to contribute no more than about 5% to the ground state intensity.) A summary of the ^{93}Nb levels observed in this work is given in Table II, along with the results obtained from $^{92}Zr(^3He,d)^4$ and Coulomb excitation.[13] The excitation energies from (α,t) agree, in general, with those from the $(^3He,d)$ reaction.[4]

The 1.08 MeV $\ell = 4$ level is populated about 1/20 as strongly as the ground state, in agreement with the spectroscopic factors measured by Cates, Ball, and Newman.[4] The 1.29 MeV level, however, is too strong to be the $\ell = 1$ level assigned in Ref. 4. Rogers et al.[13] observed a level at 1.295 MeV which agreed equally well with either a $\frac{7}{2}^+$ or $\frac{9}{2}^-$ assignment. More recently, Stelson et al.[23] investigated the Coulomb excitation of ^{93}Nb with α-particles and ^{16}O ions and obtained a tentative $\frac{9}{2}^+$ state at 1.297 MeV. The strength of the (α,t) state seen here tends to confirm the Coulomb excitation assignments[13,23] of a high-spin state at 1.29 MeV in ^{93}Nb. The angular distributions of the 0.0, 1.08, and 1.29 MeV levels are shown in Fig. 2. The shapes of the three curves are all quite similar but, as was indicated in Ref. 7, the ℓ-dependence of (α,t) angular distributions is not very pronounced.

In the $^{92}Mo(\alpha,t)^{93}Tc$ experiment of Ref. 7, a group of strong levels was observed at an excitation energy of about 6 MeV. A $^{92}Mo(^3He,d)$ experiment[5] indicated a possible $\ell = 5$ assignment for one of these levels. A similar group

of levels occurs in the $^{92}Zr(\alpha,t)^{93}Nb$ data at about 4.5 MeV (see Fig. 1). The appearance of rather strong levels at this excitation energy suggests a high angular-momentum assignment, but it is not possible to assign ℓ-values from our data.

B. $^{94}Zr(\alpha,t)^{95}Nb$

A triton spectrum of the $^{94}Zr(\alpha,t)^{95}Nb$ reaction is shown in Fig. 3. The resolution is 50 keV FWHM. A summary of the ^{95}Nb levels observed in this work is given in Table III, along with the results of the β-decay[12] and $^{94}Zr(^{3}He,d)$[4] experiments. The excitation energies obtained from our data agree well with those reported by Cates, Ball, and Newman.[4]

Information on the pair of $\frac{7}{2}^{+}$ states at 724.23 and 756.74 keV observed by Brahmavar and Hamilton[12] was, unfortunately, impossible to obtain from our data. The 0.74 and 0.82 MeV levels (both assigned $\ell = 1$ in Ref. 4) are not adequately resolved in our spectra (see Fig. 3) and the doublet also contains a contribution from the $^{92}Zr(\alpha,t)^{93}Nb$ (g.s.) peak due to an isotopic impurity in the target. The existence of an $\ell = 1$ level at 0.77 MeV was also reported in the $^{96}Mo(d,^{3}He)$ experiment of Ohnuma and Yntema,[3] in agreement with the $^{94}Zr(^{3}He,d)$ results.[4] The intensities of both the 0.74 and 0.82 MeV levels appear somewhat large compared to the 0.25 MeV state based on the $\ell = 1$ spectroscopic factors of Ref. 4. However, in view of the experimental problems it is difficult to know whether this discrepancy is real.

The level observed in our data at 1.00 MeV appears to be populated relatively more strongly than was true for the $(^{3}He,d)$ experiment, which is consistent with the $\ell = 3$ assignments made in Refs. 3 and 4.

The highest level reported in the $^{94}Zr(^{3}He,d)$ data,[4] at 1.26 MeV, was believed to be a high angular momentum (ℓ = 3,4) state. As can be seen from Fig. 3, this state (level 6), at 1.27 MeV in our data, is strongly excited in the (α,t) reaction. Similarly, the levels 8 and 11, at 1.65 and 2.10 MeV, are also strongly populated. The 1.65 MeV level contains a contribution from the $^{90}Zr(\alpha,t)^{91}Nb$ (g.s.) impurity peak amounting to about 1/3 of the total intensity. The 2.10 MeV level appears broad at all angles and is probably a doublet. Angular distributions for the 0.0, 1.27, 1.65, and 2.10 MeV levels (Fig. 4) are all very similar. The angular distribution of the 1.65 MeV level has been corrected for the presence of ^{91}Nb (g.s.) tritons.

Figure 3 also shows a group of fairly strong excited states at about 4.5 MeV in ^{95}Nb. The strength of these levels in the (α,t) reaction suggests a high angular momentum assignment, although no definite ℓ-value can be assigned from our data.

C. $^{91}Zr(\alpha,t)^{92}Nb$

This data corresponds to that mentioned as "Ref. 14" in a previous paper.[7] A triton spectrum of the $^{91}Zr(\alpha,t)^{92}Nb$ reaction at $\theta_\ell = 15°$ is shown in Fig. 5. The resolution is 65 keV FWHM. The spectrum is dominated by the multiplet of levels whose configuration is predominantly[24] $(\pi g_{9/2}, \nu d_{5/2})_{2^+ \rightarrow 7^+}$, i.e., by the capture of a $g_{9/2}$ proton. Insofar as this simple picture is correct, two results are required: the cross sections of the states should be proportional to $(2J_f + 1)$ and the total (α,t) strength of the multiplet should be the same as that for the $g_{9/2}$ ground state of ^{91}Nb. The angular distributions of the five strong levels (the 0.478 and 0.498 MeV states were not resolved in our data) are shown in Fig. 6. The 0.27 and 0.36 MeV levels were separated

by means of a Gaussian peak fitting program. The similarity to the $^{90}Zr(\alpha,t)^{91}Nb$ (g.s.) angular distribution[7] is clear. The $(2J_f + 1)$ dependence of the integrated cross sections is given in Table IV. The results are consistent with the recent $^{93}Nb(d,t\gamma)^{92}Nb$ experiment of Bhatia, Daehnick, and Canada[24] and the $^{91}Zr(^3He,d)$ results of Ball and Cates.[25]

As mentioned earlier, the absolute target thicknesses (and therefore absolute cross sections) are not well known, but a check on the relative thicknesses of the ^{90}Zr and ^{91}Zr targets is possible due to the appearance of the $^{90}Zr(\alpha,t)^{91}Nb$ (g.s.) peak as an impurity in the $^{91}Zr(\alpha,t)$ spectra. Since the integrated cross section for this impurity peak is only about 6% higher than that obtained from the ^{90}Zr target (using the nominal target thicknesses given in Table I), it is possible to compare the $^{90}Zr(\alpha,t)$ and $^{91}Zr(\alpha,t)$ cross sections directly. The total integrated cross section of the five levels (from $\theta_{c.m.} = 15.7$ to $57.4°$) is 2.4 mb. The cross section for the $^{90}Zr(\alpha,t)^{91}Nb$ (g.s.) reaction (with the ^{90}Zr target) over the same angular range is 2.7 mb. The agreement indicates that this multiplet does, in fact, contain most of the $\pi g_{9/2}$ strength.

A list of the levels observed in the $^{91}Zr(\alpha,t)^{92}Nb$ reaction is given in Table V, along with the $^{91}Zr(^3He,d)^{92}Nb$ results.[4] As can be seen in Fig. 5, there are few strong excited states except for the 1.40 and 1.63 MeV levels, both of which are assigned $\ell = 1$ in the $(^3He,d)$ work.[4] Weak levels at these energies were also reported in the $^{93}Nb(d,t)$ reaction,[24] but both were assigned $\ell = 0$ transitions. Since the neutron pickup and proton stripping reactions would not, in general, be expected to populate the same levels, the discrepancy is probably due to the formation of different states.

A weak group of levels appears at about 3.5 MeV in both the (α,t) and (^{3}He,d) data, which would be consistent with the formation of a [^{91}Nb(3.37 MeV) ⊗ $\nu d_{5/2}$] multiplet at this energy. A similar group of levels at about 5 MeV which is populated rather strongly in (α,t) might be associated with a [^{91}Nb(4.77 MeV) ⊗ $\nu d_{5/2}$] multiplet. Both multiplets would be expected based on the strong states observed in the ^{90}Zr(α,t)^{91}Nb reaction.[7]

D. ^{90}Zr(α,d)^{92}Nb

A spectrum of the ^{90}Zr(α,d)^{92}Nb reaction at $\theta_\ell = 20°$ is shown in Fig. 7. The resolution is 50 keV (FWHM). A summary of the levels observed in this work is given in Table VI. Except for the low-lying ($\pi g_{9/2}$, $\nu d_{5/2}$) multiplet in ^{92}Nb, very few levels are populated in both the ^{91}Zr(α,t) and ^{90}Zr(α,d) reactions. This implies that most of the states observed in (α,d) do not contain appreciable $\nu d_{5/2}$ strength. The 1.08 MeV level appears (weakly) in <u>all</u> reactions leading to ^{92}Nb, including the ^{93}Nb(d,t) experiment;[24] thus, it probably has a rather complicated structure. The level density is too high to make detailed comparisons between the ^{91}Zr(α,t) and ^{90}Zr(α,d) data, but the (α,d) levels at 2.46, 2.81, and 4.83 MeV may correspond to levels seen in the single-nucleon transfer (cf. Table V).

The selectivity of the (α,d) reaction is evident from the relative intensities of the levels belonging to the ($\pi g_{9/2}$, $\nu d_{5/2}$) multiplet (see Sec. III C). The 7^+ (g.s.) is populated much more strongly than the other states in the multiplet; it is about 20 times stronger than the 4^+, 6^+ doublet at 0.50 MeV. The only level populated as strongly as the ground state (7^+) is No. 13, at 2.58 MeV. Angular distributions for the ground and 2.58 MeV states are shown

in Fig. 8. The higher excited states tend to have rather structureless angular distributions, differing from one another only in slope. The ground state (7^+), however, does exhibit some oscillatory behavior. Similar structure was reported[18] for the $0^+ \rightarrow 7^+$ transition in the $^{40}Ca(\alpha,d)^{42}Sc$ reaction although the oscillations were attributed to the presence of a nearby 1^+ level in that case. This $0^+ \rightarrow 7^+$ (L = 6) pattern (Fig. 8) does appear to reproduce in the other examples studied in this work (see below).

E. $^{92}Mo(\alpha,d)^{94}Tc$

A spectrum of the $^{92}Mo(\alpha,d)^{94}Tc$ reaction at $\theta_\ell = 20°$ is shown in Fig. 9. The resolution is 65 keV (FWHM). The spectrum is quite similar to that of the $^{90}Zr(\alpha,d)^{92}Nb$ reaction (Fig. 7): only two levels are strongly excited, the ground and 2.68 MeV states. A summary of the levels observed in this work is given in Table VII.

Relatively little is known about the ^{94}Tc level scheme. The ground state is known to be a 6^+ or 7^+ based on the observed isomeric transition from the 107 keV 2^+ level and the allowed β-decay of ^{94g}Tc to the 2.4232 MeV 6^+ level in ^{94}Mo.[26] The observed strength of the ground state in (α,d) is inconsistent with a 6^+ assignment since the 6^+ should be at least 20 times weaker than the 7^+ based on the $^{90}Zr(\alpha,d)^{92}Nb$ results (Sec. III D). Also, the angular distribution of the ground state (Fig. 10) is identical with that of the 7^+ ^{92}Nb (g.s.). Thus, the (α,d) results indicate clearly that 7^+ is the correct assignment for the ^{94}Tc ground state, in agreement with the predictions of Bhatt and Ball[8] and Vervier.[10]

The only other member of the $[\pi(g_{9/2})^3_{9/2}, \nu d_{5/2}]$ multiplet expected in (α,d) is the 5^+, which is predicted[8,10] at an excitation energy of about 0.2 MeV.

The most reasonable possibility for the 5^+ state in ^{94}Tc is the (α,d) level at 0.21 MeV. The intensity of this state relative to the ground state is 0.25, in agreement with the value of $\sigma(5^+)/\sigma(7^+) = 0.25$ from the ^{90}Zr(α,d) results. The angular distribution of the 0.21 MeV level (Fig. 11) is similar to that of the 0.36 MeV 5^+ level in ^{92}Nb. The ^{94}Mo(p,nγ) experiment[27] indicates two closely spaced levels, at 209 and 216 keV, either (or both) of which could be responsible for the observed (α,d) strength of the 0.21 MeV state. However, the ^{90}Zr(α,d) results (Table VI) indicate that only the 5^+ and possibly the 3^+ levels will give strong (α,d) transitions.

In previous (α,d) studies[18-20] preferential population of a level in a given mass region was shown to be due to capture of a proton-neutron pair into one specific shell-model configuration (e.g., $(d_{5/2})^2_{5^+}$ or $(g_{9/2})^2_{9^+}$). The identification of the level in various final nuclei was made on the basis of: (a) strong population in (α,d), (b) similar angular distribution, and (c) regular dependence of the Q-value for forming the level on mass number. In this case the strongest (α,d) states are those at 2.58 MeV in ^{92}Nb and 2.68 MeV in ^{94}Tc. The strengths of these states (relative to their 7^+ ground states) are almost identical. Moreover, the angular distribution of the ^{94}Tc 2.68 MeV level (Fig. 10) is very similar to that of the ^{92}Nb 2.58 MeV level. Possible shell-model configurations for these levels will be discussed below.

F. ^{92}Zr(α,d)^{94}Nb

A spectrum of the ^{92}Zr(α,d)^{94}Nb reaction at $\theta_\ell = 20°$ is shown in Fig. 12. The resolution is 50 keV (FWHM). As with the ^{90}Zr and ^{92}Mo targets (Figs. 7 and 9) only two levels, at 0.08 and 2.42 MeV, are strongly populated. A summary of the levels observed in this work is given in Table VIII.

In contrast to the situation for ^{94}Tc, the levels in ^{94}Nb have been studied extensively, both by ^{93}Nb(n,γ)[28,29] and ^{93}Nb(d,p).[30,31] The 79 keV level is believed to be the 7^+ state based on its relative intensity in (d,p)[30] and its weak decay to the ground state.[28] [The ground state was given a tentative 7^+ assignment by Moorhead and Moyer,[31] but the excitation energy determined here of 0.08 ± 0.03 MeV argues against this assignment. Calculations of the ^{94}Nb level scheme[8,10,28-30] all give 6^+ as the lowest level.] The 5^+ level of the $[\pi g_{9/2}, \nu(d_{5/2})^3_{5/2}]$ multiplet, at 0.113 MeV,[28,31] was not resolved from the 7^+ in our data. The angular distribution of the 0.08 MeV level in (α,d) is less structured than those of the 7^+ levels in ^{92}Nb or ^{94}Tc (Figs. 8 and 10) but is accounted for rather well (Fig. 13) by assuming a $7^+ + 5^+$ doublet with relative intensities the same as those observed in ^{90}Zr(α,d).

The 2.42 MeV state has an angular distribution (Fig. 13) similar to that of the ^{92}Nb 2.58 MeV level. Its strength relative to the 7^+ level is consistent with those obtained for the strong states in ^{92}Nb and ^{94}Tc. Based on (α,d) systematics this level should have the same configuration as the ^{92}Nb 2.58 MeV and ^{94}Tc 2.68 MeV states.

G. ^{94}Zr(α,d)^{96}Nb

A spectrum of the ^{94}Zr(α,d)^{96}Nb reaction at $\theta_\ell = 20°$ is shown in Fig. 14. The resolution is 50 keV (FWHM). The low-lying levels in ^{96}Nb were studied with the ^{96}Zr(^{3}He,t)^{96}Nb reaction by Comfort et al.[32] They obtained excellent agreement with the predictions of the Pandya transformation, which relates the energies of the $[\pi g_{9/2}, (\nu d_{5/2})^{-1}]$ particle-hole multiplet in ^{96}Nb to those of the $[\pi g_{9/2}, \nu d_{5/2}]$ particle-particle multiplet in ^{92}Nb. In particular the 7^+ level, which should be strong in (α,d), was observed[32] at 233 ± 5 keV in ^{96}Nb. Preliminary results from the ^{96}Zr(p,nγ)^{96}Nb reaction[33] are in agreement with those from (^{3}He,t).

Since recent measurements[34,35] of the ^{96}Nb → ^{96}Mo β-decay indicate a mass excess for ^{96}Nb different from that in the published Q-value tables,[36] we used an energy scale obtained by fitting (α,d) data on the ^{90}Zr, ^{92}Zr, and ^{92}Mo targets (along with light impurities) to determine the energy of the 7^+ level. An excitation energy of 0.26 ± 0.03 MeV was obtained using the Q-value consistent with the β-decay data[34] while the published[36] Q-value, -12.3342 MeV, gives an excitation energy of about 0.30 MeV. Thus, based on our data, the mass excess of ^{96}Nb obtained from the β-decay, which is 37 keV more positive than that from Ref. 36, seems preferred. In order to minimize the effect of shifts between the various targets, the final calibration was done using a ^{94}Zr(α,d)^{96}Nb Q-value of -12.371 MeV (inferred from Ref. 34) and assuming an excitation energy for the 7^+ level of 0.233 MeV as given by Comfort et al.[32] The excitation energies determined in this manner are given in Table IX along with the ^{96}Zr(^{3}He,t)^{96}Nb results. Our energies depend on the choice of Q-value and may have a systematic error if the Q-value of our calibration state is incorrect, but this causes only small errors ($\lesssim$ 20 keV) over the energy range covered in Table IX.

As with the other Zr isotopes only two levels are strongly populated. Angular distributions of these levels, at 0.23 and 2.38 MeV, are shown in Fig. 15. The 0.23 MeV level has a shape consistent with the 7^+ assignment made by Comfort et al.[32] and the 2.38 MeV level is similar in shape to the ^{92}Nb 2.58 MeV state.

H. ^{91}Zr(α,d)^{93}Nb

A spectrum of the ^{91}Zr(α,d)^{93}Nb reaction at θ_ℓ = 20° is shown in Fig. 16. The resolution is 65 keV (FWHM). A summary of the levels seen in this work is given in Table X.

It is interesting to compare the low-lying levels seen in the $^{91}Zr(\alpha,d)^{93}Nb$ data to those seen in $^{92}Zr(\alpha,t)^{93}Nb$ (Sec. III A and Table II) and Coulomb excitation.[13] The ground state ($\frac{9}{2}^+$) is populated quite weakly in (α,d) compared with the dominant $\pi g_{9/2}$ capture in (α,t). A stronger group of levels appears at about 1.3 MeV in the (α,d) data. These levels have been assigned[13] spins of: 0.952 MeV ($\frac{13}{2}^+$), 1.337 MeV ($\frac{17}{2}^+$), 1.492 MeV ($\frac{9}{2}^+$, $\frac{11}{2}^+$, $\frac{13}{2}^+$), and 1.507 MeV ($\frac{9}{2}^+$, $\frac{11}{2}^+$, $\frac{13}{2}^+$). Shell model calculations of the ^{93}Nb level scheme[8,10] predict low-lying $\frac{11}{2}^+$, $\frac{13}{2}^+$, $\frac{15}{2}^+$, and $\frac{17}{2}^+$ levels whose wave functions are of the type $[\pi g_{9/2}, \nu(d_{5/2})^2_{J_n}]_J$. From the $^{90}Zr(\alpha,d)^{92}Nb$ results (Sec. III D) it seems clear that only those levels having appreciable amplitudes of the type $[(\pi g_{9/2}, \nu d_{5/2})_{7^+}, \nu d_{5/2}]$ and $[(\pi g_{9/2}, \nu d_{5/2})_{5^+}, \nu d_{5/2}]$ will be populated strongly, since the 7^+ and 5^+ have the most favorable structure for the (α,d) reaction. The strongest levels, then, should be the $\frac{17}{2}^+$ and $\frac{15}{2}^+$ since these must contain only 5^+, 6^+, or 7^+ couplings of the transferred ($\pi g_{9/2}$, $\nu d_{5/2}$) pair. The $\frac{17}{2}^+$ state, which is the "stretched" configuration of the $[\pi g_{9/2}, \nu(d_{5/2})^2]$ multiplet, should be populated only through the 7^+ coupling, i.e., it should be the same transfer as that for the $^{90}Zr(\alpha,d)^{92}Nb$ (g.s.) reaction. (The 6^+ is not expected to contribute appreciably to the cross section either experimentally (Sec. III D) or theoretically.[15]) This prediction is borne out by the angular distribution of the 1.33 MeV level (Fig. 17) which has the same shape as that from the $^{90}Zr(\alpha,d)^{92}Nb$ (g.s.) reaction. Also, the 1.33 MeV level is the strongest of the low-lying levels seen in $^{91}Zr(\alpha,d)$. Thus, our data tends to substantiate the identification of the $\frac{17}{2}^+$ level at 1.337 MeV made in Ref. 13.

The $\frac{15}{2}^+$ level is predicted[8,10] to lie slightly higher than the $\frac{17}{2}^+$ level. Based on our results the 1.48 MeV level would seem to be a reasonable candidate,

although Rogers et al.[13] assigned ($\frac{9}{2}^+$, $\frac{11}{2}^+$, $\frac{13}{2}^+$) to both the 1.492 and 1.507 MeV levels. Both the 1.48 MeV and 0.96 MeV levels have angular distributions (Fig. 17) which can be "fit" with the assumption of $7^+ + 5^+$ contributions similar to those from the ground and 0.36 MeV states of ^{92}Nb.

At about 4 MeV a second strong group of states appears in the ^{91}Zr(α,d) data (Fig. 16). The angular distributions of these levels, at 3.54, 3.84, 3.93, 4.06, 4.21, and 4.52 MeV, are all similar to that of the 2.58 MeV level in ^{92}Nb and probably correspond to the same proton-neutron transfer. Angular distributions of two of these levels (3.54 and 4.52 MeV) are shown in Fig. 18. The splitting between the two multiplets is about 2.7 MeV. This is consistent with a simple "weak coupling" picture of these groups of states, although it is very unlikely that the levels do not mix with other available configurations in ^{93}Nb.

IV. DISCUSSION

A. (α,t)

There has been great interest recently in the spectroscopic information obtainable from heavy-ion induced transfer reactions. A study of the (^{16}O, ^{15}N) reaction on all of the even Zr isotopes has recently been reported.[37] The Zr(^{16}O, ^{15}N) reactions were observed to strongly favor the capture of a $g_{9/2}$ proton by an undisturbed Zr core. (The ground state $\pi g_{9/2}$ cross section was in all cases at least a factor of 3 larger than that for any other state.) This result indicates a preference for large angular momentum transfers similar to that shown by the (α,t) reaction on the same targets (see Ref. 7 and Sec. III A and B). The Zr(^{16}O, ^{15}N) results[37] were compared to the Zr(^{3}He,d) results of Cates, Ball, and Newman[4] in order to determine which levels were populated by single-particle transitions. Several other states, not seen or seen weakly in (^{3}He,d), were interpreted as possible core-excited levels of the type [Zr(2^+) ⊗ $\pi g_{9/2}$] or [Zr(3^-) ⊗ $\pi g_{9/2}$]. Since the angular momentum aspects of the (^{16}O, ^{15}N) reaction appear to be similar to those of the (α,t) reaction, it seems reasonable to compare the results of the two in order to determine which levels might be populated due to their high spin rather than due to core excitation. A summary of the core-excited levels seen in (^{16}O, ^{15}N) compared to nearby levels seen in (α,t) is given in Table XI. As can be seen from this comparison, essentially all of the levels seen in the heavy-ion work[37] also appear in our data.

In ^{93}Nb there is good evidence[23] that some of the low-lying states do have [$^{92}Zr(2^+)$ ⊗ $\pi g_{9/2}$] components. However, for the 1.08 MeV $\frac{9}{2}^+$ level, the $^{92}Zr(^{3}He,d)^{4}$ and ^{92}Zr(α,t) strengths (relative to the ground state $\ell = 4$ transition) are identical. This implies that two step excitations in (α,t) are no

more important than those in (^{3}He,d). The appearance of these states in both (α,t) and (^{16}O, ^{15}N), then, may be due to the high angular momentum transfer in the heavy ion reaction rather than to a two step collective excitation. Very possibly both the single-particle and collective aspects of these strong levels are contributing to the heavy ion cross sections, but we suggest that "elimination" of those states having mainly single-particle character be done by comparison with (α,t) as well as (^{3}He,d) data in order to better reproduce the momentum matching conditions of the heavy ion experiments. In the present case, the appearance of these levels (Table XI) as fairly strong (α,t) transitions certainly casts some doubt on the mechanism of their excitation in (^{16}O, ^{15}N).[37]

B. (α,d)

As mentioned previously, the three criteria used for selecting (α,d) states of the same configuration are: (a) large cross section in (α,d), (b) similar angular distribution, and (c) regular dependence of the Q-value for forming the level, Q_f, on mass number. We have shown that requirements (a) and (b) are met by the strong (α,d) levels seen in this work. A summary of the Q-values for formation of these levels in (α,d) is given in Table XII. Unfortunately, neither of the strong (α,d) groups seen here displays the regular Q_f vs. mass dependence observed previously.[18-20] It is clear that the lack of regularity in Q_f is not due to a failure of the reaction to selectively populate specific shell model configurations, since the 7^+ levels (which correspond to the energies labeled E_1 in Table XII) have been identified in all but one case by other reactions.[24,28,32] Since both groups of strong levels show the same Q-value behavior (i.e., the relative energy difference between the two groups remains nearly constant at about 2.4 MeV), it seems reasonable to associate the levels

listed as E_2 in Table XII with a specific shell model state in spite of the irregular Q_f vs. A dependence.

One possible explanation for the anomalous behavior of the 7^+ levels is that both the $g_{9/2}$ proton and $d_{5/2}$ neutron are entering partially filled shells and thus the wave function is somewhat different in each case. For example, in ^{92}Nb the 7^+ is mainly a "simple" two-particle $(\pi g_{9/2}, \nu d_{5/2})_{7^+}$ state, while in ^{94}Tc the wave function is $[(\pi g_{9/2})^3_{9/2}, \nu d_{5/2}]_{7^+}$ and in ^{94}Nb it is $[\pi g_{9/2}, (\nu d_{5/2})^3_{5/2}]_{7^+}$. This was not the case for the levels observed in previous (α,d) studies[18-20] except for the 5^+ levels in ^{22}Na and ^{26}Al, which are in a deformed mass region. Consistent with this hypothesis is the fact that the Q_f-vs. A dependence for the Zr isotopes alone is similar to that observed previously. From evidence presented below it seems likely that the higher group of levels also contains a $\pi g_{9/2}$ configuration, which would account for its behavior being similar to that of the 7^+ levels.

C. Shell Model Calculations

In this mass region there are a number of high-spin proton-neutron states which might be strongly populated in (α,d). One of these configurations, $(\pi g_{9/2}, \nu d_{5/2})_{7^+}$, is already known in the nuclei studied here. As expected, this configuration is selectively populated in the (α,d) reaction in all cases. Other possible high-spin states, to which the higher (α,d) group might correspond, are $(\pi g_{9/2}, \nu h_{11/2})_{10^-}$, $(\pi g_{9/2}, \nu g_{7/2})_{8^+}$, $(d_{5/2})^2_{5^+}$, $(\pi g_{7/2}, \nu d_{5/2})_{6^+}$, $(g_{7/2})^2_{7^+}$, and $(\pi g_{7/2}, \nu h_{11/2})_{9^-}$.

In order to determine which possibilities are reasonable, simple shell model calculations have been performed using the code PHYLLIS.[38] The method

of calculation is outlined by Brody and Moshinsky.[39] The calculations were done using a Gaussian potential employed by True in calculating the ^{14}N spectrum:[40]

$$V_{TE} = -52 \exp(-0.2922\ r^2)\ (\text{MeV})$$

$$V_{SE} = \frac{V_{TE}}{1.6}$$

$$V_{SO} = V_{TO} = 0 \quad .$$

The oscillator parameter, ν, was determined by requiring that the calculated residual interaction, V_{RES}, for the $(\pi g_{9/2}, \nu d_{5/2})_{7^+}$ state be the same as the empirical value for the ^{92}Nb ground state, -0.679 MeV. This yielded a value of $\nu = 0.156\ fm^{-2}$. In previous calculations[20] the oscillator parameter was calculated according to the formula

$$\nu = \frac{2n + \ell + 3/2}{R^2} = \frac{2n + \ell + 3/2}{(r_0 \cdot A^{1/3})^2} \quad .$$

Our value of the oscillator parameter would correspond to a radius parameter $r_0 = 1.32$ fm.

Matrix elements and excitation energies obtained with this oscillator parameter are given in Table XIII. The single-particle energies required to calculate the excitation energies are taken from single-nucleon transfer data[2,41] and are listed in Table XIV. Figure 19 illustrates the results of the calculation for the states belonging to the $(\pi g_{9/2}, \nu d_{5/2})$ multiplet. The ordering and splitting of these levels are reproduced reasonably well by the calculations.

Based on the results in Table XIII, it seems clear that the most likely configurations for the 2.58 MeV level in ^{92}Nb are $(\pi g_{9/2}, \nu h_{11/2})_{10^-}$ and $(\pi g_{9/2}, \nu g_{7/2})_{8^+}$. (The predicted excitation energies for states containing an $h_{11/2}$ neutron are lower limits because not all of the $\ell = 5$ strength was observed in Ref. 41 and the remainder presumably lies at higher excitation energies in ^{91}Zr.) The large single-particle energies for excited proton states make it extremely unlikely that a state with other than a $g_{9/2}$ proton would appear at such a low excitation energy in ^{92}Nb. As can be seen from Table XIII, the calculated interaction energies are quite similar for all of the high-spin configurations considered here. Thus, the predicted excitation energies depend strongly on the single-particle energies but are not particularly sensitive to the choice of oscillator parameters.

One problem in doing these calculations arises because the $h_{11/2}$ level is in a different oscillator shell than the other levels. From the formula above this should correspond to a different oscillator parameter. To see what effect this has on the predicted interaction energies, a modified calculation with different oscillator parameters for the two particles was performed using the code NAOMI.[38] The generalized transformation brackets can be expanded in terms of products of standard Moshinsky brackets[39] using a formula derived by Gal.[42] The Talmi integrals must also be modified slightly because the transformation to relative coordinates requires a "redefined" oscillator parameter

$$\nu = \frac{\nu_1 \nu_2}{\nu_1 + \nu_2} \quad ,$$

where ν_1 and ν_2 are the oscillator parameters for particles 1 and 2. The oscillator parameter for the $h_{11/2}$ neutron was obtained by assuming the shell dependence indicated above:

$$\nu' = \frac{2n' + \ell' + 3/2}{2n + \ell + 3/2} \times \nu$$

$$= \frac{6.5}{5.5} \times 0.156$$

$$= 0.184 \text{ fm}^{-2} \quad .$$

The results of this calculation are included in Table XIII. The larger $h_{11/2}$ oscillator parameter has the effect of increasing the residual interaction matrix elements by about 15%. The predicted excitation energies are, therefore, decreased by about 200 keV.

D. (α,d) Structure Factors

Shell model calculations (Sec. IV C) suggest that the best candidates for the higher level observed in the (α,d) data are $(\pi g_{9/2}, \nu h_{11/2})_{10^-}$ and $(\pi g_{9/2}, \nu g_{7/2})_{8^+}$. Such high spin states are kinematically favored in (α,d), because the momentum matching for the reaction is best for large L transfers. [The classical angular momentum transfer $\vec{Q} \times \vec{R} \approx 8.$] The structure of these high-spin states is also favorable for the (α,d) reaction, since they contain relatively large amounts of the [target core + deuteron] configuration required[14] for strong population in (α,d). Structure factors for these levels have been tabulated by Glendenning[15] and are listed in Table XV. The probability of finding the favored ^3S correlation for the transferred pair (with center of mass angular momentum L) is given by

$$P_L = \sum_N G_{NL}^2 \quad .$$

This probability, weighted by 2J + 1, is also given in Table XV. Since no kinematic effects are included in this probability, the ratios in Table XV cannot be interpreted as relative cross sections even if the wave functions are adequately described by these simple configurations. However, the relative probabilities do serve to indicate, for example, that the $(\pi g_{9/2}, \nu g_{7/2})_{8^+}$ would probably be weaker than the $(\pi g_{9/2}, \nu h_{11/2})_{10^-}$ (assuming the L = 8 and L = 9 kinematics are similar) and that either of these states would be comparable in strength to the $(\pi g_{9/2}, \nu d_{5/2})_{7^+}$ level.

V. CONCLUSIONS

A. (α,t)

A search for high-spin proton levels in ^{92,93,95}Nb has been made with the (α,t) reaction. Based on relative strengths compared with the (^{3}He,d) data of Cates, Ball, and Newman,[4] the following excited states are believed to be populated with $\ell > 2$ transitions: ^{92}Nb(≈ 5 MeV multiplet); ^{93}Nb(1.08, 1.29, ≈ 4.5 MeV); and ^{95}Nb(1.27, 1.65, 2.10, ≈ 4.5 MeV). The multiplets near 5 MeV in these nuclei are at an excitation energy where $\ell = 5$ proton strength has been tentatively identified in the ^{92}Mo(^{3}He,d)^{93}Tc reaction by Kozub and Youngblood.[5] The (2J + 1) dependence of the ($\pi g_{9/2}$, $\nu d_{5/2}$) multiplet in ^{92}Nb has been investigated with the ^{91}Zr(α,t)^{92}Nb reaction. The results are in good agreement with the recent spin determinations from the ^{93}Nb(d,tγ) reaction.[24]

A comparison of our results with the Zr(^{16}O, ^{15}N) data[37] indicates that most of the levels populated in the heavy-ion induced proton transfer also appear in (α,t). This may be due to the heavy ion kinematics, which appears to favor population of the $\ell = 4$ ground states in these nuclei similar to the preference shown in (α,t). We suggest that a comparative study of the (α,t) and heavy ion proton stripping will provide a convenient means of observing the "momentum matching" aspects of the heavy ion experiments.

B. (α,d)

We have shown that the tendency of the (α,d) reaction to selectively populate high-spin states continues in the Zr-Mo region. The $(\pi g_{9/2}, \nu d_{5/2})_{7^+}$ transfer is strong in all of the Nb isotopes studied here. The ground state of ^{94}Tc has been shown to be a 7^+ by this work, based on its strength and angular distribution, and the ^{94}Tc 0.21 MeV level is a probable 5^+ state. Levels of the

$[\pi g_{9/2}, (\nu d_{5/2})^2]$ configuration have been observed in ^{93}Nb. In particular, the $\frac{17}{2}^+$ assignment[13] for the 1.337 MeV level is in agreement with our results and a candidate for the $\frac{15}{2}^+$ level has been observed at 1.48 MeV in ^{93}Nb.

A second strong (α,d) state was observed in all the nuclei studied here at about 2.4 MeV higher excitation energy than the 7^+ level. (See Table XII for a summary of the preferentially populated (α,d) states.) Simple shell model calculations suggest that $(\pi g_{9/2}, \nu g_{7/2})_{8^+}$ and $(\pi g_{9/2}, \nu h_{11/2})_{10^-}$ are the most likely high-spin configurations expected in this energy region. The structure factors for (α,d)[14,15] indicate that either of these levels would be strong in the (α,d) reaction. The neutron single-particle energies from ^{92}Mo(d,p)[31] suggest that the $\nu g_{7/2}$ centroid may be significantly lower than the $\nu h_{11/2}$ centroid in ^{93}Mo. This argues for a 10^- assignment for the ^{94}Tc 2.68 MeV level, since the observed $\nu g_{7/2}$ centroid (1.58 MeV) would correspond to a <u>repulsive</u> residual interaction if the 2.68 MeV level is associated with the $(\pi g_{9/2}, \nu g_{7/2})_{8^+}$ configuration. Unfortunately, a great deal of the spectroscopic strength of both $\nu g_{7/2}$ and $\nu h_{11/2}$ has not yet been observed so no firm conclusions can be reached at this time.

ACKNOWLEDGMENTS

We would like to thank E. A. McClatchie, C. C. Lu, J. D. Sherman, D. L. Hendrie, and J. Mahoney for help with the experiment and C. Maples for allowing us to use his computer codes LORNA and DERTAG for some of the data analysis. We are also indebted to C. Ellsworth for preparing the targets.

FOOTNOTES AND REFERENCES

*Work performed under the auspices of the U. S. Atomic Energy Commission.

1. J. Picard and G. Bassani, Nucl. Phys. A131, 636 (1969).
2. G. Vourvopoulos, R. Shoup, J. C. Fox, and J. B. Ball, in Nuclear Isospin, ed. by J. D. Anderson, S. D. Bloom, J. Cerny, and W. W. True, (Academic Press, Inc., New York, 1969), p. 205.
3. H. Ohnuma and J. L. Yntema, Phys. Rev. 176, 1416 (1968).
4. M. R. Cates, J. B. Ball, and E. Newman, Phys. Rev. 187, 1682 (1969).
5. R. L. Kozub and D. H. Youngblood, Phys. Rev. C 4, 535 (1971).
6. K. T. Knöpfle, M. Rogge, C. Mayer-Böricke, J. Pederson, and D. Burch, Nucl. Phys. A159, 642 (1970).
7. M. S. Zisman and B. G. Harvey, Phys. Rev. C, to be published.
8. K. H. Bhatt and J. B. Ball, Nucl. Phys. 63, 286 (1965).
9. N. Auerbach and I. Talmi, Nucl. Phys. 64, 458 (1965).
10. J. Vervier, Nucl. Phys. 75, 17 (1966).
11. K. Hesse and E. Finckh, Nucl. Phys. A141, 417 (1970).
12. S. M. Brahmavar and J. H. Hamilton, Phys. Rev. 187, 1487 (1969).
13. V. C. Rogers, L. E. Beghian, F. M. Clikeman, F. Hofman, and S. Wilensky, Nucl. Phys. A142, 100 (1970).
14. N. K. Glendenning, Phys. Rev. 137, B102 (1965).
15. N. K. Glendenning, Lawrence Radiation Laboratory Report UCRL-18270 (unpublished).
16. J. Cerny, B. G. Harvey, and R. H. Pehl, Nucl. Phys. 29, 120 (1962).
17. R. H. Pehl, E. Rivet, J. Cerny, and B. G. Harvey, Phys. Rev. 137, B114 (1965).
18. E. Rivet, R. H. Pehl, J. Cerny, and B. G. Harvey, Phys. Rev. 141, 1021 (1966).

19. C. C. Lu, M. S. Zisman, and B. G. Harvey, Phys. Letters 27B, 217 (1968).

20. C. C. Lu, M. S. Zisman, and B. G. Harvey, Phys. Rev. 186, 1086 (1969).

21. M. S. Zisman, E. A. McClatchie, and B. G. Harvey, Phys. Rev. C 2, 1271 (1970).

22. F. S. Goulding, D. A. Landis, J. Cerny, and R. H. Pehl, Nucl. Instr. Methods 31, 1 (1964).

23. P. H. Stelson, R. L. Robinson, W. T. Milner, F. K. McGowan, and M. A. Ludington, Bull. Am. Phys. Soc. 16, 619 (1971).

24. T. S. Bhatia, W. W. Daehnick, and T. R. Canada, Phys. Rev. C 3, 1361 (1971).

25. J. B. Ball and M. R. Cates, Phys. Letters 25B, 126 (1967).

26. N. K. Aras, E. Eichler, and G. G. Chilosi, Nucl. Phys. A112, 609 (1968).

27. A. S. M. de Jesus and W. L. Rautenbach, Nucl. Phys. A138, 626 (1969).

28. U. Gruber, R. Koch, B. P. Maier, O. W. B. Schult, J. B. Ball, K. H. Bhatt, and R. K. Sheline, Nucl. Phys. 67, 433 (1965).

29. E. T. Jurney, H. T. Motz, R. K. Sheline, E. B. Shera, and J. Vervier, Nucl. Phys. A111, 105 (1968).

30. R. K. Sheline, R. T. Jernigan, J. B. Ball, K. H. Bhatt, Y. E. Kim, and J. Vervier, Nucl. Phys. 61, 342 (1965).

31. J. B. Moorhead and R. A. Moyer, Phys. Rev. 184, 1205 (1969).

32. J. R. Comfort, J. V. Maher, G. C. Morrison, and J. P. Schiffer, Phys. Rev. Letters 25, 383 (1970).

33. S. Cochavi and D. B. Fossan, Bull. Am. Phys. Soc. 16, 620 (1971).

34. S. Antman, H. Pettersson, and Y. Grunditz, Nucl. Phys. A110, 289 (1968); S. Antman, Y. Grunditz, A. Johansson, B. Nyman, H. Pettersson, and B. Svahn, Z. Physik 233, 275 (1970).

35. H. W. Taylor, B. Singh, R. J. Cox, and A. H. Kukoc, Z. Physik 239, 42 (1970).

36. C. Maples, G. W. Goth, and J. Cerny, Nucl. Data A2, 429 (1966).

37. R. J. Nickles, V. I. Manko, P. R. Christensen, and F. D. Becchetti, Phys. Rev. Letters 26, 1267 (1971).

38. Shell model matrix element code written by M. S. Zisman, (unpublished).

39. T. A. Brody and M. Moshinsky, Tables of Transformation Brackets, (Gordon and Breach Science Publishers, Inc., New York, 1967).

40. W. W. True, Phys. Rev. 130, 1530 (1963).

41. C. R. Bingham and M. L. Halbert, Phys. Rev. C 2, 2297 (1970).

42. A. Gal, Ann. Phys. (N.Y.) 49, 341 (1968).

Table I. Target Composition.

Target	Nominal Thickness (mg/cm^2)	Zr Targets Isotopic Abundance (At. %)				
		^{90}Zr	^{91}Zr	^{92}Zr	^{94}Zr	^{96}Zr
^{90}Zr	0.20	97.8	0.95	0.65	0.49	< 0.1
^{91}Zr	0.30	4.95	91.85	2.51	0.62	0.07
^{92}Zr	0.40	2.86	1.29	94.57	1.15	0.14
^{94}Zr	0.25	2.08	0.69	0.92	96.07	0.24

		Mo Target						
		^{92}Mo	^{94}Mo	^{95}Mo	^{96}Mo	^{97}Mo	^{98}Mo	^{100}Mo
^{92}Mo	0.30	98.27	0.46	0.37	0.26	0.13	0.27	0.25

Table II. Levels Observed in the $^{92}Zr(\alpha,t)^{93}Nb$ Reaction at 50 MeV.

	(α,t)		(^{3}He,d)[a]			Coulomb Excitation[b]	
No.	Levels Observed[c] (MeV)	Intensity[d] (mb)	Levels Observed[e] (MeV)	ℓ_p[f]	C^2S	Levels Observed[g] (MeV)	J^π
1	0.0	2.672	0.0	4	0.79	0.0	$9/2^+$
			0.029 ± 0.005	1	0.53	0.028	$1/2^-$
2	0.69	0.079	0.685	1	0.07		
						0.742	$7/2^+$
						0.808	$3/2^-$
3	0.80 ± 0.03	0.070	0.807	2	0.06	0.809	$5/2^+$
4	0.95	0.064[h]				0.952	$13/2^+$
			0.97 ± 0.01	1	0.006	0.980	$9/2^+$
5	1.08	0.144	1.08	4	0.04	1.080	$7/2^+$
6	1.29	0.304	1.29	1	0.05	1.295	$(7/2^+,9/2^-)$
			1.33	(2)	(0.04)	1.337	$(17/2^+)$
7	1.37 ± 0.03	WEAK					
						1.465	$(3/2^+,5/2^-)$
						1.492	$(9/2^+,11/2^+,13/2^+)$
						1.507	$(9/2^+,11/2^+,13/2^+)$
						1.528	
8	1.57 ± 0.03	0.028	1.57	1	0.02		
9	1.67	0.055	1.66	2	0.008		
			1.71	2	0.006		
10	2.00 ± 0.03	0.021[i]					
11	2.15 ± 0.03	0.125	2.18	2	0.03		

(continued)

Table II. (continued)

No.	(α,t) Levels Observed[c] (MeV)	(α,t) Intensity[d] (mb)	(^{3}He,d)[a] Levels Observed[e] (MeV)	(^{3}He,d)[a] ℓ_p[f]	(^{3}He,d)[a] C^2S	Coulomb Excitation[b] Levels Observed[g] (MeV)	Coulomb Excitation[b] J^π
12	2.30 2.36	0.087	2.32	2	0.03		
13	2.48 ± 0.03	0.089	2.52	(0)			
14	2.59 ± 0.03	0.038	2.59	2	0.02		
15	2.81	0.067					
16	2.98	0.091[j]					
17	3.15	0.054					
18	3.50	0.066[i]					
19	3.72 ± 0.03	0.038[i]					
20	3.84 ± 0.03	0.044[i]					
21	4.23	0.072[i]					
22	4.34	0.043[i]					
23	4.46	0.120[i]					
24	4.56	0.080[i]					
	(4.65)	--					
25	4.70 ± 0.03	0.067[i]					
26	4.81 ± 0.03	0.084[i]					
27	5.00 ± 0.03	0.066[i]					
28	5.34 ± 0.04	0.071[i]					
29	5.49 ± 0.04	--					

(continued)

Table II. (continued)

[a]Ref. 4.

[b]Ref. 13.

[c]Excitation energy ±20 keV except as noted.

[d]Integrated from $\theta_{c.m.}$ = 12.5 to 52.2° except as noted.

[e]Excitation energy ±15 keV except as noted.

[f]All ℓ = 1 transitions assumed $p_{3/2}$ except for 0.029 MeV. All ℓ = 2 transitions assumed $d_{5/2}$. All ℓ = 4 transitions assumed $g_{9/2}$.

[g]Excitation energy ±2 keV.

[h]Integrated from $\theta_{c.m.}$ = 15.7 to 52.2°.

[i]Integrated from $\theta_{c.m.}$ = 12.5 to 36.7°.

[j]Integrated from $\theta_{c.m.}$ = 12.5 to 47.1°.

Table III. Levels Observed in the $^{94}Zr(\alpha,t)^{95}Nb$ Reaction at 50 MeV.

	(α,t)		(^{3}He,d)[a]			^{95}Zr Decay[b]	
No.	Levels Observed[c] (MeV)	Intensity[d] (mb)	Levels Observed[e] (MeV)	ℓ_p[f]	C^2S	Levels Observed[g] (MeV)	J^π
1	0.0	2.540	0.0	4	0.86	0.0	$9/2^+$
2	0.25	0.081	0.26	1	0.34	0.23470	$1/2^-$
3	0.74	0.104	0.73	1	0.045	0.72423	$(7/2)^+$
						0.75674	$(7/2)^+$
4	0.82	0.103	0.80	1	0.077		
5	1.00	0.038	0.99	3	0.030		
			1.20	1	0.022		
6	1.27	0.198	1.26	(3,4)			
7	1.43	0.054					
8	1.65	0.139[h]					
9	1.72	0.079[i]					
10	1.81 }	{ 0.15					
	1.90 }	{					
11	2.10	0.212					
12	2.42	0.090					
13	2.54	0.023[j]					
14	2.66	0.032[j]					
15	2.79	0.030[j]					
16	2.92	0.036[j]					
17	3.11	0.062[j]					

(continued)

Table III. (continued)

	(α,t)		$(^3He,d)^a$			^{95}Zr Decay[b]	
No.	Levels Observed[c] (MeV)	Intensity[d] (mb)	Levels Observed[e] (MeV)	ℓ_p^f	C^2S	Levels Observed[g] (MeV)	J^π
18	3.51	0.035[k]					
19	3.90	0.073[j]					
20	4.05	0.041[j]					
21	4.16	0.057[j]					
22	4.36	0.125[j]					
23	4.52	0.147[j]					
24	4.61	0.060[j]					
25	4.83	0.102[j]					
26	5.20	0.068[ℓ]					
27	5.36	--					
28	5.77	--					

[a] Ref. 4.

[b] Ref. 12.

[c] Excitation energy ± 20 keV except as noted.

[d] Integrated from $\theta_{c.m.}$ = 12.5 to 52.1° except as noted.

[e] Excitation energy ±15 keV.

[f] All ℓ = 1 levels except 0.26 MeV assumed $p_{3/2}$. The 0.99 MeV level assumed $f_{5/2}$.

(continued)

Table III. (continued)

[g]Excitation energy ±0.2 keV or less.

[h]Corrected for $^{90}Zr(\alpha,t)^{91}Nb$ (g.s.) impurity.

[i]Integrated from $\theta_{c.m.}$ = 15.7 to 52.1°.

[j]Integrated from $\theta_{c.m.}$ = 12.5 to 33.6°.

[k]Integrated from $\theta_{c.m.}$ = 12.5 to 26.1°.

[ℓ]Integrated from $\theta_{c.m.}$ = 12.5 to 31.4°.

Table IV. $(2J_f + 1)$ Dependence of the $(\pi g_{9/2}, \nu d_{5/2})$ Multiplet in the $^{91}Zr(\alpha,t)^{92}Nb$ Reaction.

Level[a] (MeV)	J_f^{π} [a]	σ[b] (mb)	σ_R[c] (mb)	Ratio[d]
0.0	7^+	0.590	0.236	1.00
0.135	2^+	0.190	0.228	0.97
0.285	3^+	0.255	0.219	0.93
0.356	5^+	0.492	0.269	1.14
0.478	4^+	0.899	0.245	1.04
0.498	6^+			

[a]Taken from Ref. 24.

[b]Integrated from $\theta_{c.m.} = 15.7$ to $57.4°$.

[c]
$$\sigma_R = \frac{(2J_i + 1)}{(2J_f + 1)} \times \sigma = \frac{6\sigma}{(2J_f + 1)}$$

[d]Relative to ground state reduced cross section.

Table V. Levels Observed in the $^{91}Zr(\alpha,t)^{92}Nb$ Reaction at 50 MeV.

	(α,t)		(^{3}He,d)[a]		
No.	Levels Observed[b] (MeV)	Intensity[c] (mb)	Levels Observed (MeV)	ℓ_p	C^2S
1	0.0	0.590	0.0	4	0.75
2	0.14	0.190	0.130 ± 0.005	4	0.74
			0.225	1	0.40
3	0.28	0.255	0.285	4	0.81
4	0.36	0.492	0.350	4	0.67
			0.388	1	0.34
5	0.49	0.899	0.478	4	1.00
			0.503	4	0.91
6	1.10	0.017[d]	1.09 ± 0.01	1	
			1.32	1	
7	1.40	0.059	1.42	1	
8	1.63	0.055	1.64	1	
			1.67	1	
			1.72	1	
9	1.83	0.048[e]			
10	2.49	0.044[f]			
11	2.80	0.038[e]			
12	2.94	0.032[f]			
13	3.36	--			
14	3.53	0.025[g]			
15	3.66	0.060[f]			
16	4.83 ± 0.10	--			
17	4.93 ± 0.10	--			
18	5.21 ± 0.10	--			

[a]Ref. 4.

[b]Excitation energies ±20 keV except as noted.

(continued)

Table V. (continued)

[c]Integrated from $\theta_{c.m.}$ = 15.7 to 57.4° except as noted.

[d]Integrated from $\theta_{c.m.}$ = 15.7 to 36.5°.

[e]Integrated from $\theta_{c.m.}$ = 15.7 to 52.3°.

[f]Integrated from $\theta_{c.m.}$ = 15.7 to 47.1°.

[g]Integrated from $\theta_{c.m.}$ = 15.7 to 31.4°.

Table VI. Levels Observed in the $^{90}Zr(\alpha,d)^{92}Nb$ Reaction at 50 MeV.

No.	Levels Observed[a] (MeV)	Intensity[b] (mb)
1	0.0	0.278
2	0.13	WEAK
3	0.21	WEAK
4	0.28	0.025
5	0.36	0.069
6	0.49	0.01
7	1.08	0.022
8	1.75	0.03
9	2.03	0.019
10	2.15	0.051
11	2.28	0.097
12	2.47	0.166[c]
13	2.58	0.345
14	2.81	0.047[c]
15	3.72	0.057
16	3.81	0.040
17	3.92	0.053
18	4.45	0.04[d]
19	4.83	0.05[d]
20	5.62	0.124
21	(6.0 ± 0.1)	--

[a]Excitation energy error ±30 keV except as noted.

[b]Integrated from $\theta_{c.m.}$ = 12.4 to 56.8° except as noted.

[c]Integrated from $\theta_{c.m.}$ = 12.4 to 51.7°.

[d]Integrated from $\theta_{c.m.}$ = 12.4 to 31.1°.

Table VII. Levels Observed in the $^{92}Mo(\alpha,d)^{94}Tc$ Reaction at 50 MeV.

No.	Levels Observed[a] (MeV)	Intensity[b] (mb)
1	0.0	0.336
2	0.10	0.040
3	0.21	0.083
4	0.34	WEAK
5	0.45	0.027
6	0.93	0.040
7	1.22	0.039
8	1.30	0.042
9	1.41	0.040
10	1.64	0.045
11	1.74	0.139
12	2.14	WEAK
13	2.35	0.109[c]
14	2.43	0.04[d]
15	2.68	0.446
16	2.86	0.083
17	2.95	0.06
18	3.08	0.117
19	5.07	0.09[e]
20	5.24	0.183
21	5.38	0.197

[a]Excitation energy ±30 keV.

[b]Integrated from $\theta_{c.m.}$ = 12.5 to 56.9° except as noted.

[c]Integrated from $\theta_{c.m.}$ = 12.5 to 41.6°.

[d]Integrated from $\theta_{c.m.}$ = 12.5 to 36.2°.

[e]Integrated from $\theta_{c.m.}$ = 12.5 to 51.9°.

Table VIII. Levels Observed in the $^{92}Zr(\alpha,d)^{94}Nb$ Reaction at 50 MeV.

No.	Levels Observed[a] (MeV)	Intensity[b] (mb)
1	0.08[c]	0.178[c]
2	0.32	0.01
3	0.65	0.01
4	0.95	0.04[d]
5	1.19	WEAK
6	1.25	0.049
7	1.39	0.044
8	1.65	0.027
9	1.84	0.02[d]
10	2.05	0.059
11	2.18	0.098
12	2.25	0.095
13	2.42	0.166
14	2.53	0.03[d]
15	2.69	0.060
16	2.84	0.051[e]
17	2.95	0.02[d]
18	3.7 ± 0.10	WEAK

[a]Excitation energy error ±30 keV except as noted.

[b]Integrated from $\theta_{c.m.}$ = 12.4 to 51.8° except as noted.

[c]This level is a doublet made up of the 0.078 and 0.113 MeV states. About 80% of the observed intensity should be due to the 0.078 MeV state. See text.

[d]Integrated from $\theta_{c.m.}$ = 12.4 to 36.4°.

[e]Integrated from $\theta_{c.m.}$ = 12.4 to 46.7°.

Table IX. Levels Observed in the $^{94}Zr(\alpha,d)^{96}Nb$ Reaction at 50 MeV.

	(α,d)		(^{3}He,t)[a]	
No.	Levels Observed[b] (MeV)	Intensity[c] (mb)	Levels Observed[d] (MeV)	J^π
			0.0	6^+
1	0.05	0.014[e]	0.045	5^+
			0.152	4^+
			0.191	3^+
2	0.23[f]	0.071[e]	0.233	7^+
			0.515	
			0.632	2^+
3	0.70	0.02	0.685	
4	0.83	WEAK		
			0.865	
5	1.01	0.02		
6	1.21	0.01		
7	1.41	0.07		
8	1.71	0.02		
9	1.89	0.02		
10	2.10	0.06		
11	2.24	0.04		
12	2.38	0.212[e]		
13	2.47	0.04		
14	2.73 ± 0.04	0.02		
15	2.96 ± 0.04	0.04		

[a]Ref. 32.

[b]Excitation energy error ±30 keV except as noted.

[c]Integrated from $\theta_{c.m.}$ = 12.4 to 33.2° except as noted.

[d]Relative energies ±5 keV.

(continued)

Table IX. (continued)

[e]Integrated from $\theta_{c.m.}$ = 12.4 to 51.8°.

[f]Used as a calibration point. The excitation energy of the 7^+ was obtained from Ref. 32 and the ground state Q-value, -12.371 MeV, was inferred from the β-decay Q-value of Ref. 34. (See text.)

Table X. Levels Observed in the $^{91}Zr(\alpha,d)^{93}Nb$ Reaction at 50 MeV.

No.	Levels Observed[a] (MeV)	Intensity[b] (mb)
1	0.0	0.020[c]
2	0.80	0.010
3	0.96	0.056
4	1.33	0.077
5	1.48	0.052
6	1.66	0.039
7	3.54	0.078
8	3.84	0.094[c]
9	3.93	0.050[c]
10	4.06	0.080[d]
11	4.21	0.052[d]
12	4.52	0.100

[a]Excitation energy error ±30 keV.

[b]Integrated from $\theta_{c.m.}$ = 15.5 to 56.7° except as noted.

[c]Integrated from $\theta_{c.m.}$ = 15.5 to 46.5°.

[d]Integrated from $\theta_{c.m.}$ = 15.5 to 51.7°.

Table XI. Collective Levels Observed in $Zr(^{16}O, ^{15}N)Nb$ Compared to the $Zr(\alpha,t)Nb$ Results.

Target	$(^{16}O, ^{15}N)^a$		$(\alpha,t)^b$		$(^{16}O, ^{15}N)^a$		$(\alpha,t)^b$	
	E_2[c] (MeV)	I_2[d]	E (MeV)	I[e]	E_3[f]	I_3[d]	E	I[e]
^{90}Zr	2.18	0.03	2.30	0.01	2.75	0.06	2.61	0.007
							2.77	0.003
							2.90	0.02
^{92}Zr	0.93	0.05	0.95	0.02	2.34	0.17	2.30 }	0.03
							2.36 }	
^{94}Zr	0.92	--	0.82	0.04	2.05	0.36	2.10	0.08
			1.00	0.01				

[a]Taken from Ref. 37.

[b]The ^{90}Zr results are from Ref. 7. The other isotopes are discussed in this work.

[c]Assumed $[Zr(2^+) \otimes \pi g_{9/2}]$ configuration.

[d]Ratio of differential cross section (at $\theta_\ell = 60°$) to that of ground state.

[e]Ratio of integrated cross section to that of ground state.

[f]Assumed $[Zr(3^-) \otimes \pi g_{9/2}]$ configuration.

Table XII. Q-Values of Strong (α,d) States

Final Nucleus	E_1[a] (MeV)	Q_1[b] (MeV)	E_2 (MeV)	Q_2[b] (MeV)
^{90}Y	0.69[c]	-12.79	3.11[c]	-15.21
^{92}Nb	0.0	-13.03	2.58	-15.61
^{94}Tc	0.0	-13.37	2.68	-16.05
^{94}Nb	0.08	-12.89	2.42	-15.23
^{96}Nb	0.23	-12.60	2.38	-14.75

[a] $(\pi g_{9/2}, \nu d_{5/2})_{7^+}$ states. All levels except the ^{94}Tc ground state have been assigned 7^+ by other groups. See text.

[b] Ground state Q-values taken from Ref. 36 except for ^{96}Nb, which is inferred from Ref. 34.

[c] Obtained from $^{88}Sr(\alpha,d)^{90}Y$ data, M. S. Zisman, E. A. McClatchie, and B. G. Harvey, University of California Lawrence Radiation Laboratory Report UCRL-19530, p. 100 (1970), (unpublished).

Table XIII. Summary of Shell Model Calculations for the Two-Particle States in ^{92}Nb.

Configuration	J^{π}	V_{RES} [a] (MeV)	E_x [b] (MeV)
$(\pi g_{9/2}, \nu d_{5/2})$	7^+	-0.678	0.0
$(\pi g_{9/2}, \nu h_{11/2})$	10^-	-1.263	> 2.10
		(-1.472)[c]	(> 1.89)[c]
$(\pi g_{9/2}, \nu g_{7/2})$	8^+	-1.098	2.35
$(d_{5/2})^2$	5^+	-1.129	3.75
$(\pi g_{7/2}, \nu d_{5/2})$	6^+	-0.543	5.66
$(g_{7/2})^2$	7^+	-1.268	7.70
$(\pi g_{7/2}, \nu h_{11/2})$	9^-	-0.975	> 7.90
		(-1.136)[c]	(> 7.74)[c]

[a]Calculated with a single oscillator parameter $\nu = 0.156$ fm^{-2} except as noted.

[b]Based on single-particle energies summarized in Table XIV.

[c]Calculated with oscillator parameters 0.156 and 0.184 fm^{-2} for the proton and neutron, respectively. See text.

Table XIV. Single-Particle Energies for A = 91.

	^{91}Nb[a] (MeV)	^{91}Zr[b] (MeV)
$g_{9/2}$	0.0	--
$d_{5/2}$	4.20	0.04
$s_{1/2}$	5.27	1.66
$d_{3/2}$	6.43	2.76
$g_{7/2}$	5.52	2.77
$h_{11/2}$	--	> 2.68

[a]Taken from Ref. 2.

[b]Taken from Ref. 41.

Table XV. Structure Factors for (α,d) States.

Configuration	G_{NL} [a]	P_L [b]	$(2J + 1)P_L$ [c]
$(\pi g_{9/2}, \nu d_{5/2})_{7^+}$	$G_{16} = -0.0221$, $G_{26} = 0.3140$	0.099	1.0
$(\pi g_{9/2}, \nu h_{11/2})_{10^-}$	$G_{19} = 0.4396$	0.193	2.7
$(\pi g_{9/2}, \nu g_{7/2})_{8^+}$	$G_{18} = 0.3277$	0.107	1.2
$(\pi d_{5/2}, \nu d_{5/2})_{5^+}$	$G_{14} = 0.0447$, $G_{24} = 0.0351$, $G_{34} = 0.3278$	0.111	0.8

[a] Taken from Ref. 15.

[b] $P_L = \sum_N G_{NL}^2$. P_L represents the probability of finding the appropriate ^3S correlations in the wave function.

[c] Relative to the $(\pi g_{9/2}, \nu d_{5/2})_{7^+}$ state. This ratio does not include any kinematic effects, which are also important in determining which states will be strongly populated.

FIGURE CAPTIONS

Fig. 1. Triton energy spectrum from the $^{92}Zr(\alpha,t)^{93}Nb$ reaction at $\theta_\ell = 20°$. The peak numbers correspond to excitation energies given in Table II. Peak 0 is the $^{94}Zr(\alpha,t)^{95}Nb$ (g.s.) peak resulting from an isotopic impurity.

Fig. 2. Angular distributions of tritons from the $^{92}Zr(\alpha,t)^{93}Nb$ reaction leading to the 0.0, 1.08, and 1.29 MeV levels. The solid line through each set of data points represents a smooth curve drawn through the experimental angular distribution of the ground state. Statistical errors are shown for each point.

Fig. 3. Triton energy spectrum from the $^{94}Zr(\alpha,t)^{95}Nb$ reaction at $\theta_\ell = 20°$. The peak numbers correspond to excitation energies given in Table III.

Fig. 4. Angular distributions of tritons from the $^{94}Zr(\alpha,t)^{95}Nb$ reaction leading to the 0.0, 1.27, 1.65, and 2.10 MeV levels. The solid line through each set of data points represents a smooth curve drawn through the experimental angular distribution of the ground state. Statistical errors are shown for each point.

Fig. 5. Triton energy spectrum from the $^{91}Zr(\alpha,t)^{92}Nb$ reaction at $\theta_\ell = 15°$. The peak numbers correspond to excitation energies given in Table V.

Fig. 6. Angular distributions of tritons from the $^{91}Zr(\alpha,t)^{92}Nb$ reaction leading to the 0.0, 0.135, 0.285, 0.356, and (unresolved) 0.478/0.498 MeV states. The solid line through each set of data points represents a smooth curve drawn through the experimental angular distribution of the $^{90}Zr(\alpha,t)^{91}Nb$ (g.s.) reaction from Ref. 7. Statistical errors are indicated for each point.

Fig. 7. Deuteron energy spectrum from the $^{90}Zr(\alpha,d)^{92}Nb$ reaction at $\theta_\ell = 20°$. The peak numbers correspond to excitation energies given in Table VI.

Fig. 8. Angular distributions of deuterons from the $^{90}Zr(\alpha,d)^{92}Nb$ reaction leading to the 0.0 and 2.58 MeV states. Statistical errors are shown for each point. The curves have no theoretical significance.

Fig. 9. Deuteron energy spectrum from the $^{92}Mo(\alpha,d)^{94}Tc$ reaction at $\theta_\ell = 20°$. The peak numbers correspond to excitation energies given in Table VII.

Fig. 10. Angular distributions of deuterons from the $^{92}Mo(\alpha,d)^{94}Tc$ reaction leading to the 0.0 and 2.68 MeV states. The solid lines through the data points represent smooth curves drawn through the experimental angular distributions of the $^{90}Zr(\alpha,d)^{92}Nb$ reaction leading to the ground and 2.58 MeV states (see Fig. 8). Statistical errors are shown for each point.

Fig. 11. Deuteron angular distributions from the $^{90}Zr(\alpha,d)^{92}Nb$ (0.36 MeV) and $^{92}Mo(\alpha,d)^{94}Tc$ (0.21 MeV) reactions. Statistical errors are shown for each point.

Fig. 12. Deuteron energy spectrum from the $^{92}Zr(\alpha,d)^{94}Nb$ reaction at $\theta_\ell = 20°$. The peak numbers correspond to excitation energies given in Table VIII.

Fig. 13. Angular distributions of deuterons from the $^{92}Zr(\alpha,d)^{94}Nb$ reaction leading to the 0.08 MeV and 2.42 MeV states. The solid line through the 0.08 MeV data points represents a smooth curve drawn through the experimental angular distribution of the <u>summed</u> 0.0 MeV (7^+) and 0.36 MeV (5^+) levels in $^{90}Zr(\alpha,d)^{92}Nb$. The solid line through the 2.42 MeV data points is a smooth curve drawn through the experimental angular distribution of the $^{90}Zr(\alpha,d)^{92}Nb$ (2.58 MeV) reaction. Statistical errors are shown for each point.

Fig. 14. Deuteron energy spectrum from the $^{94}Zr(\alpha,d)^{96}Nb$ reaction at $\theta_\ell = 20°$. The peak numbers correspond to excitation energies given in Table IX.

Fig. 15. Angular distributions of deuterons from the $^{94}Zr(\alpha,d)^{96}Nb$ reaction leading to the 0.23 and 2.38 MeV levels. The solid lines through the data points represent smooth curves drawn through the experimental angular distributions of the $^{90}Zr(\alpha,d)^{92}Nb$ reaction leading to the ground and 2.58 MeV states. (See Fig. 8.) Statistical errors are shown for each point.

Fig. 16. Deuteron energy spectrum from the $^{91}Zr(\alpha,d)^{93}Nb$ reaction at $\theta_\ell = 20°$. The peak numbers correspond to excitation energies given in Table X.

Fig. 17. Angular distributions of deuterons from the $^{91}Zr(\alpha,d)^{93}Nb$ reaction leading to the 0.96, 1.33, and 1.48 MeV levels. The solid lines represent smooth curves drawn through experimental angular distributions from the $^{90}Zr(\alpha,d)^{92}Nb$ reaction leading to the 7^+ (g.s.) and 5^+ (0.36 MeV) with weighting factors of: 0.96 MeV $[7^+ + 5^+]$, 1.33 MeV $[7^+]$, and 1.48 MeV $[7^+ + 2 \times (5^+)]$. (See text.) Statistical errors are shown for each point.

Fig. 18. Angular distributions of deuterons from the $^{91}Zr(\alpha,d)^{93}Nb$ reaction leading to the 3.54 and 4.52 MeV states. The solid lines represent smooth curves drawn through the experimental angular distribution of the $^{90}Zr(\alpha,d)^{92}Nb$ (2.58 MeV) reaction. (See Fig. 8.) Statistical errors are shown for each point.

Fig. 19. Comparison of the calculated and experimental spectra of the $(\pi g_{9/2}, \nu d_{5/2})$ multiplet in ^{92}Nb.

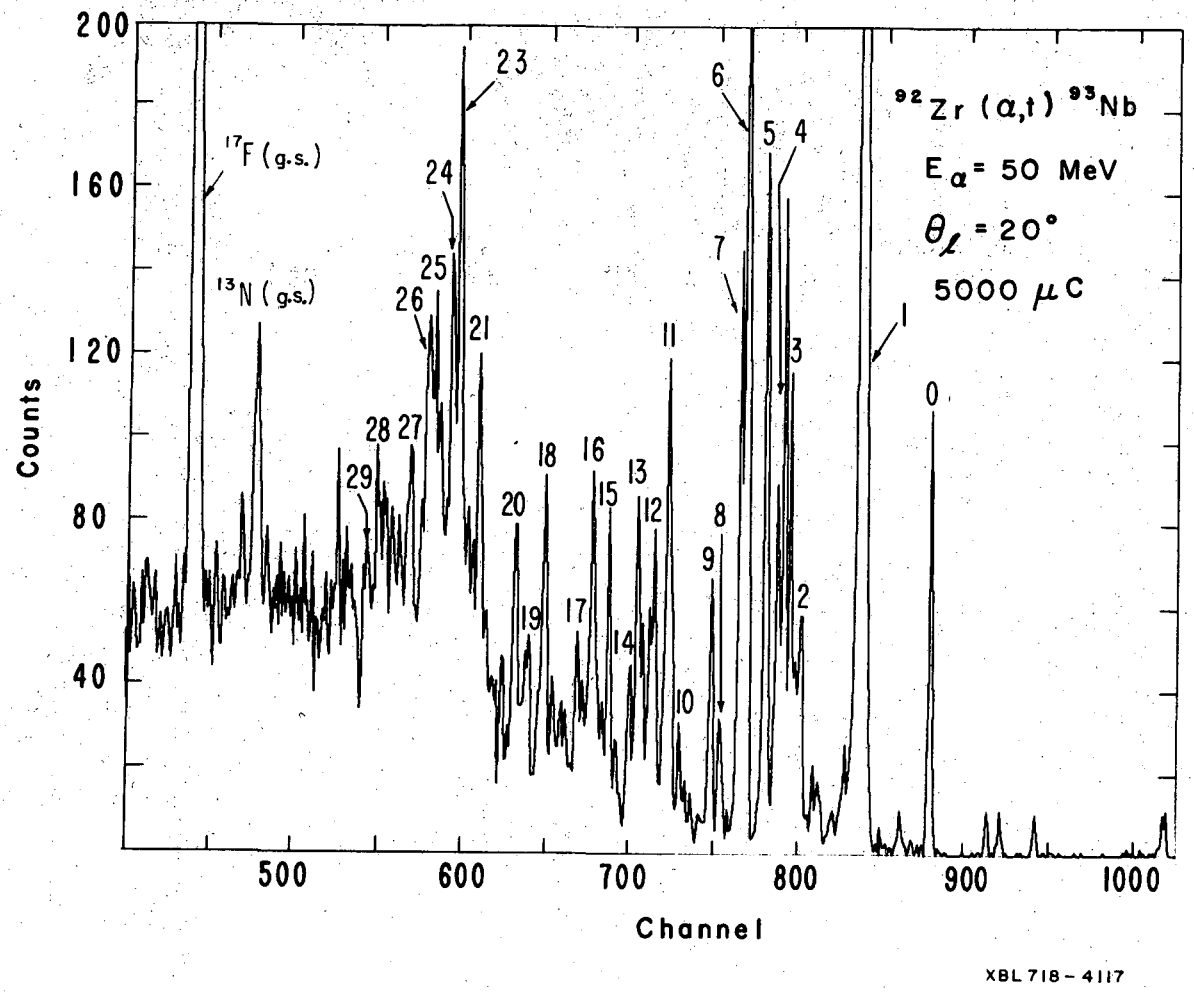

XBL 718-4117

Fig. 1

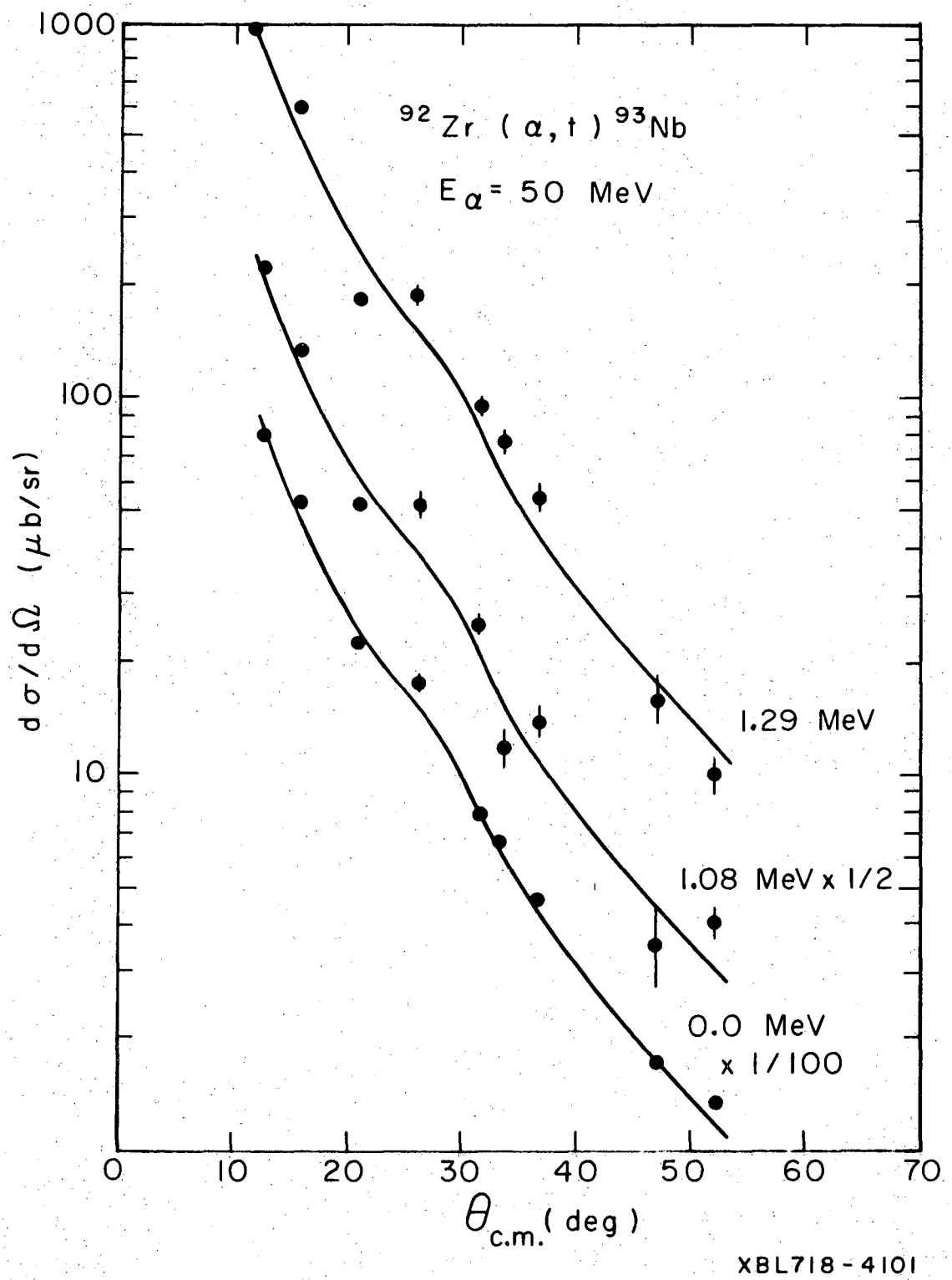
1000
100
10
0
10
20
30
40
50
60
70
^{92}Zr (α, t) ^{93}Nb
E_α = 50 MeV
1.29 MeV
1.08 MeV x 1/2
0.0 MeV
x 1/100
dσ/dΩ (μb/sr)
$\theta_{c.m.}$ (deg)
XBL718-4101

Fig. 2

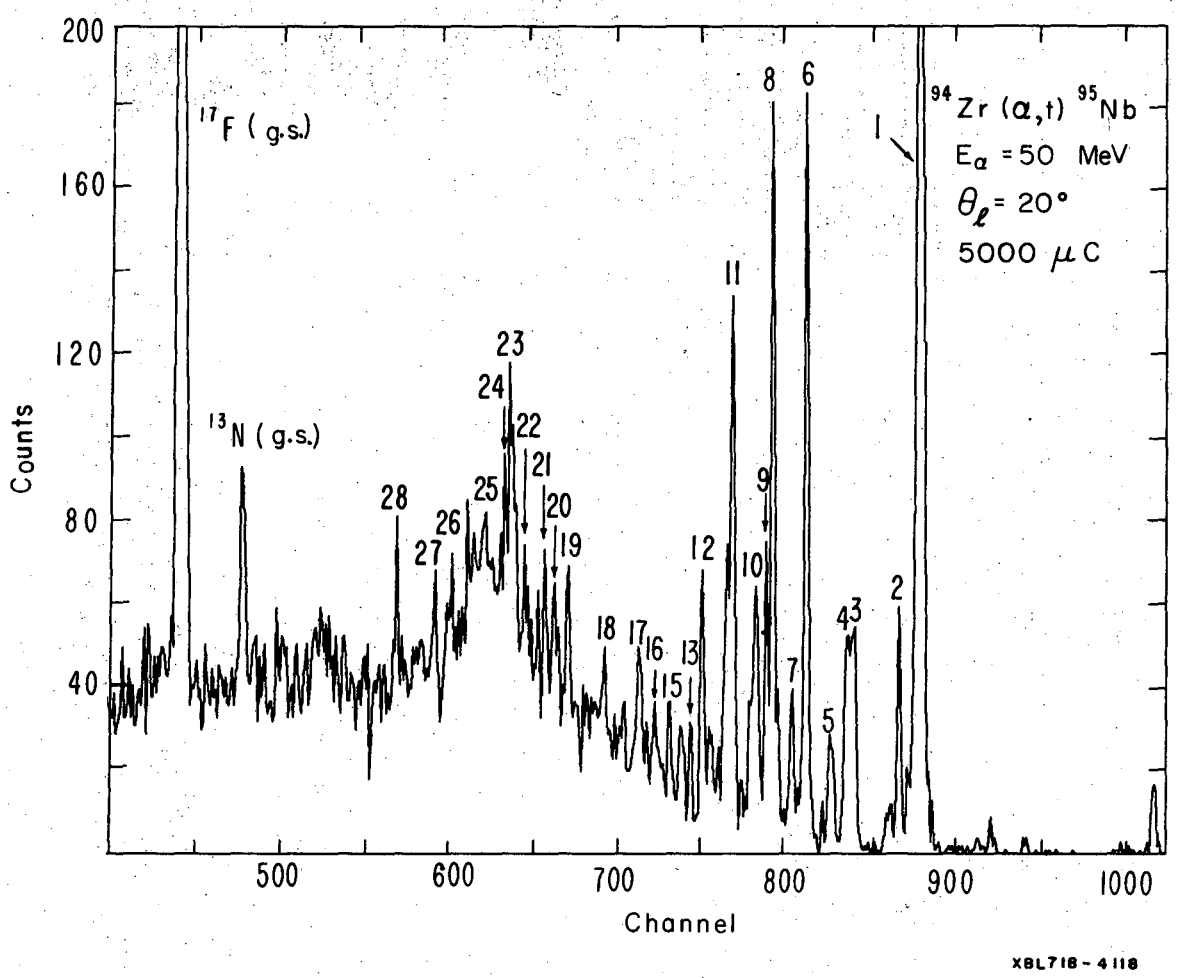
200
160
120
80
40
Counts
500
600
700
800
900
1000
Channel
^{17}F (g.s.)
^{13}N (g.s.)
^{94}Zr (α,t) ^{95}Nb
E_α = 50 MeV
θ_ℓ = 20°
5000 μC
1
2
3
4
5
6
7
8
9
10
11
12
13
15
16
17
18
19
20
21
22
23
24
25
26
27
28
XBL718-4118

Fig. 3

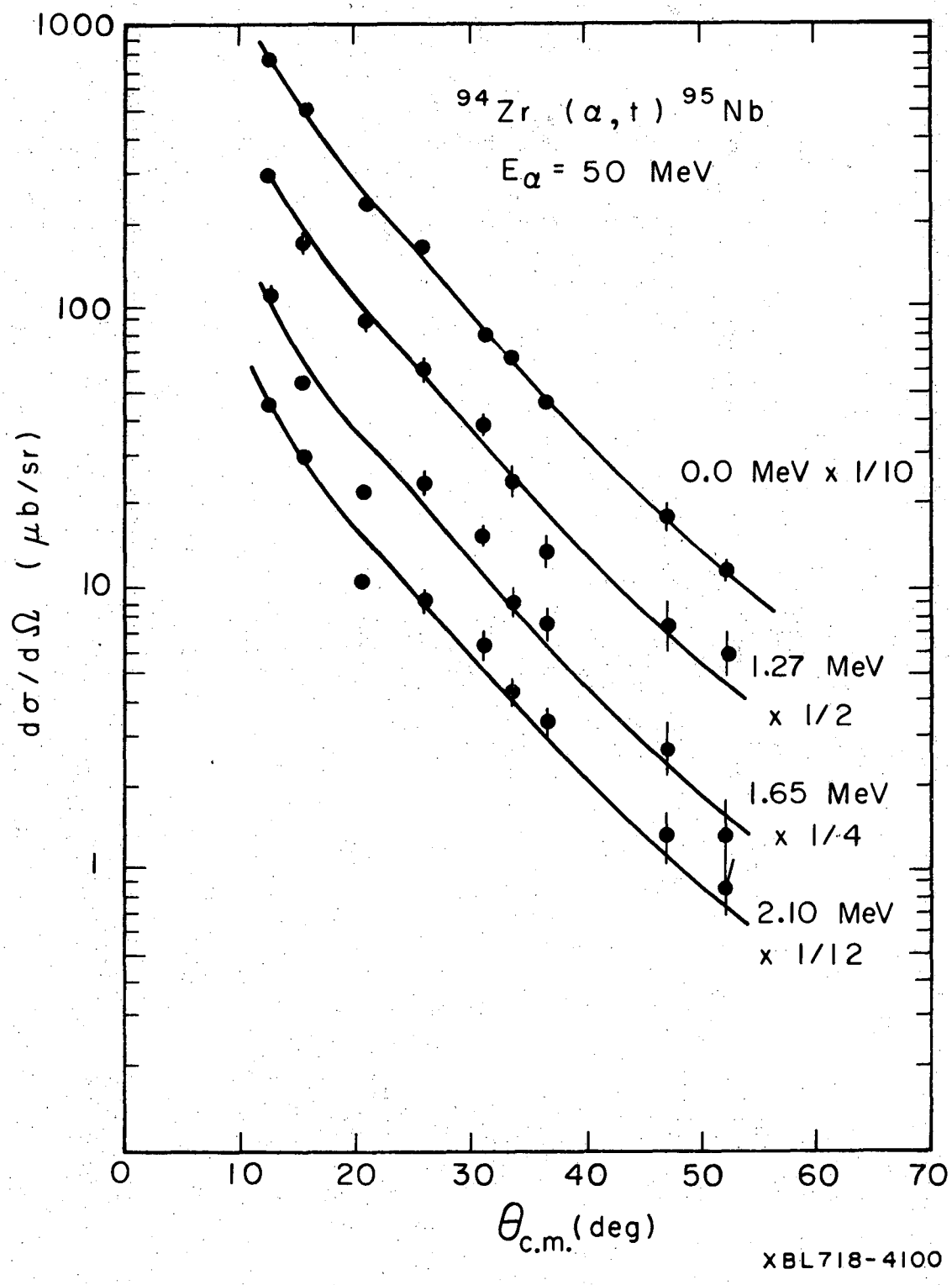
^{94}Zr (α, t) ^{95}Nb
E_α = 50 MeV
0.0 MeV x 1/10
1.27 MeV x 1/2
1.65 MeV x 1/4
2.10 MeV x 1/12
dσ/dΩ (μb/sr)
1000
100
10
1
0
10
20
30
40
50
60
70
$\theta_{c.m.}$ (deg)
XBL718-4100

Fig. 4

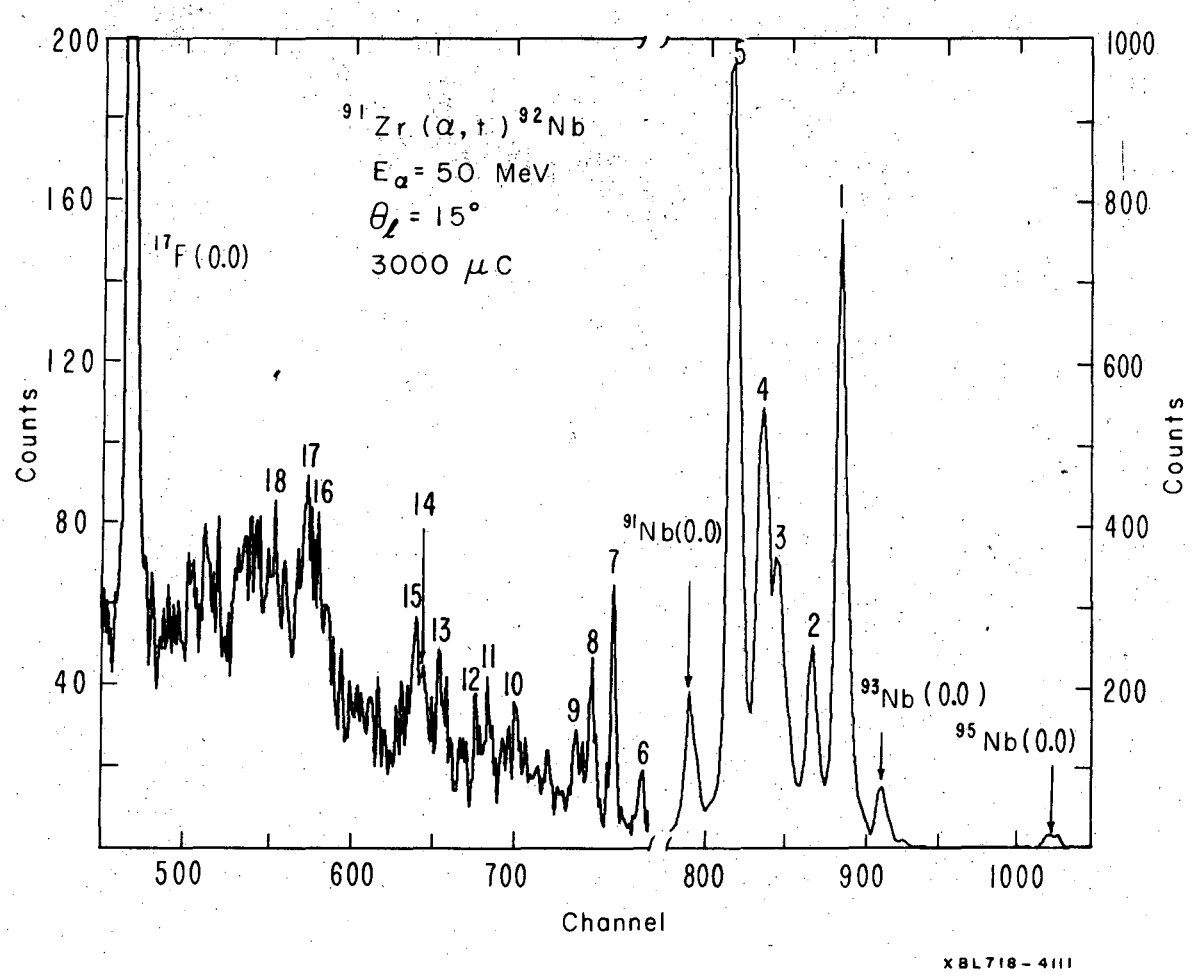
^{91}Zr (α, t) ^{92}Nb
E_α = 50 MeV
θ_ℓ = 15°
3000 μC
^{17}F (0.0)
^{91}Nb(0.0)
^{93}Nb (0.0)
^{95}Nb(0.0)
Counts
Channel
XBL718-4111

Fig. 5

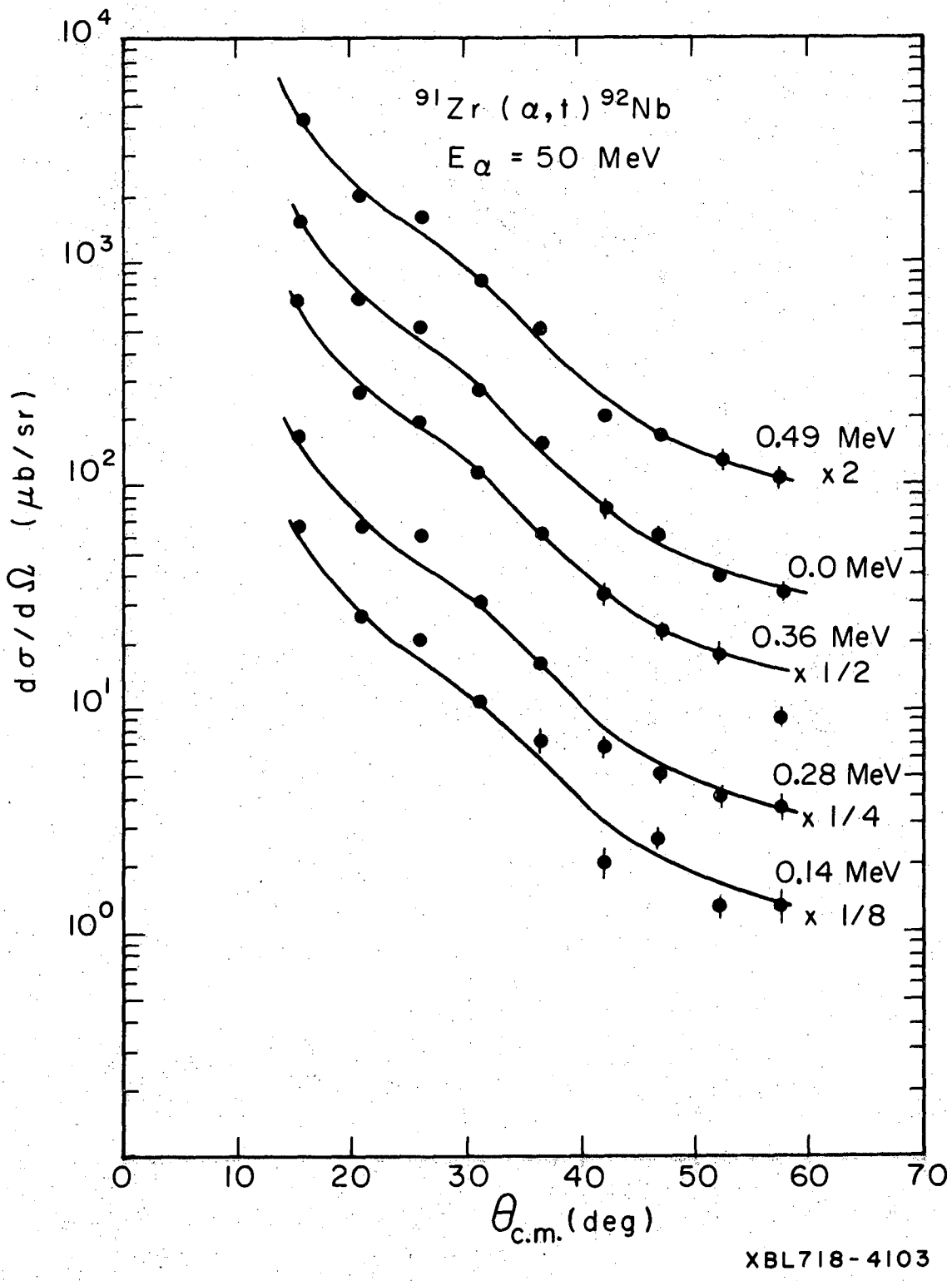
$^{91}Zr(\alpha,t)^{92}Nb$
E_α = 50 MeV
0.49 MeV
x 2
0.0 MeV
0.36 MeV
x 1/2
0.28 MeV
x 1/4
0.14 MeV
x 1/8
$d\sigma/d\Omega$ (μb/sr)
10^4
10^3
10^2
10^1
10^0
0
10
20
30
40
50
60
70
$\theta_{c.m.}$ (deg)
XBL718-4103

Fig. 6

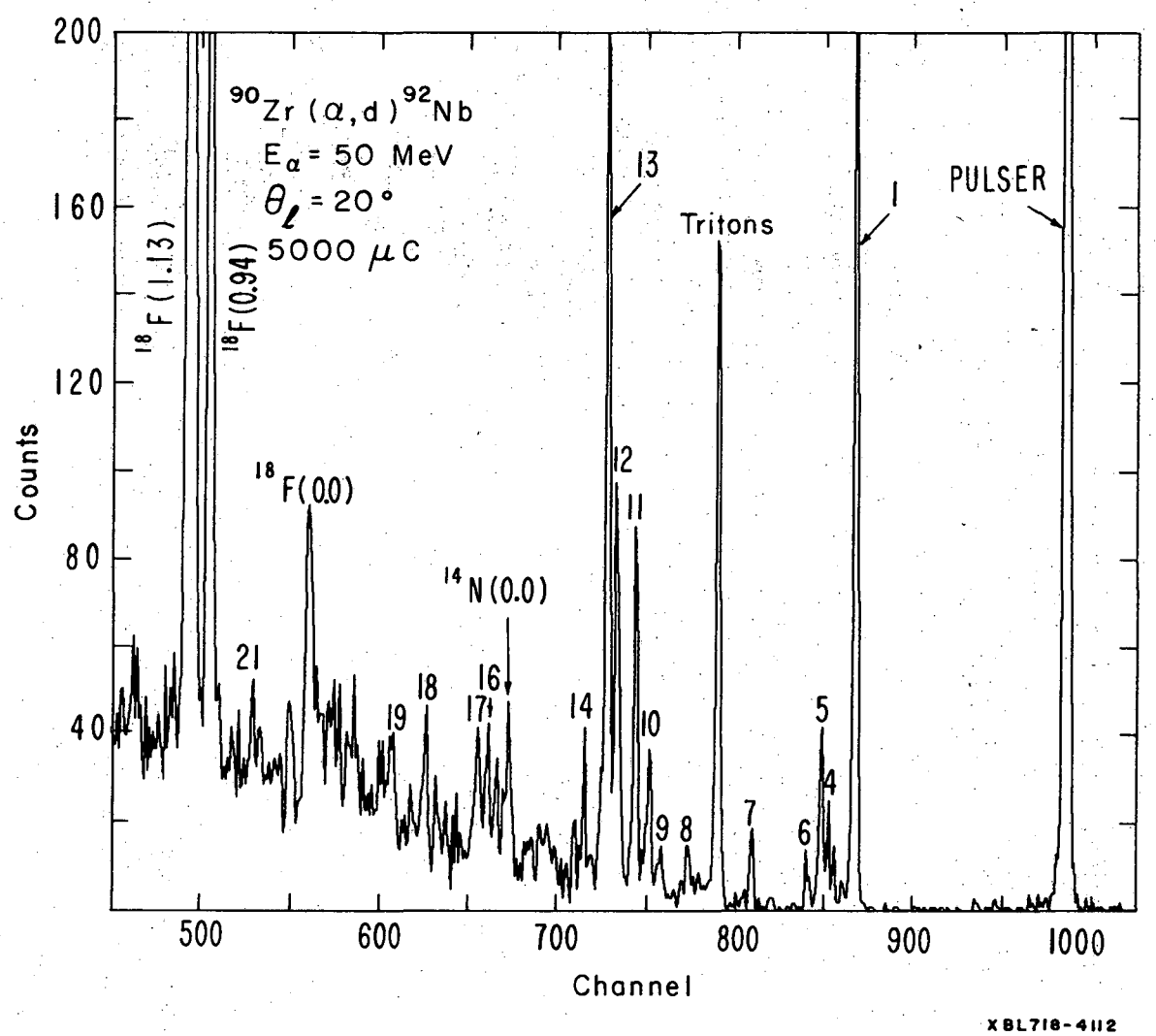
^{90}Zr (α,d) ^{92}Nb
E_α = 50 MeV
θ_ℓ = 20°
5000 μC
^{18}F (1.13)
^{18}F(0.94)
^{18}F(0.0)
^{14}N(0.0)
Tritons
PULSER
13
12
11
10
9
8
7
6
5
4
1
14
16
17
18
19
21
Counts
Channel
200
160
120
80
40
500
600
700
800
900
1000
XBL718-4112

Fig. 7

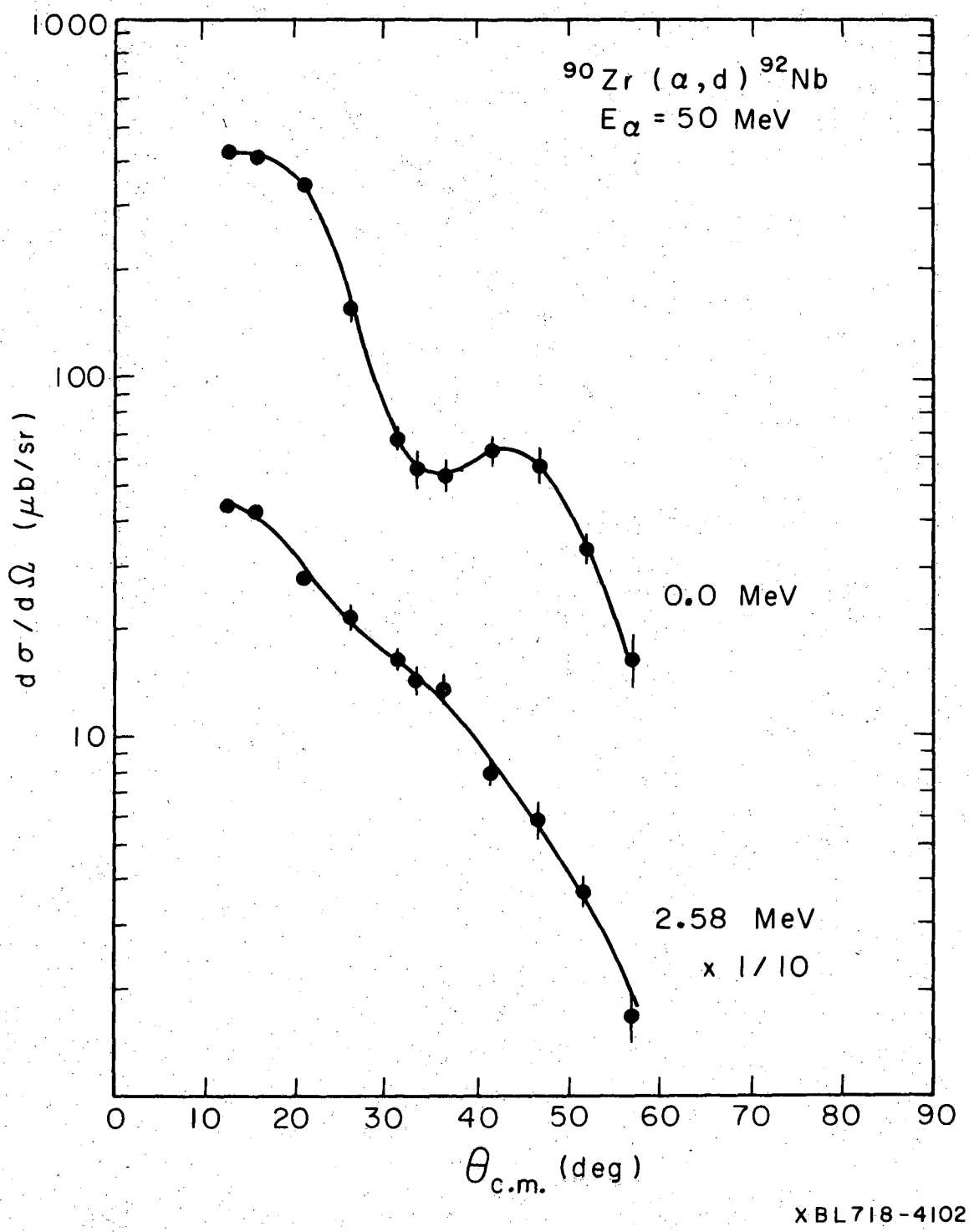
$^{90}Zr(\alpha,d)^{92}Nb$
E_α = 50 MeV
0.0 MeV
2.58 MeV
x 1/10
1000
100
10
$d\sigma/d\Omega$ (μb/sr)
0
10
20
30
40
50
60
70
80
90
$\theta_{c.m.}$ (deg)
XBL718-4102

Fig. 8

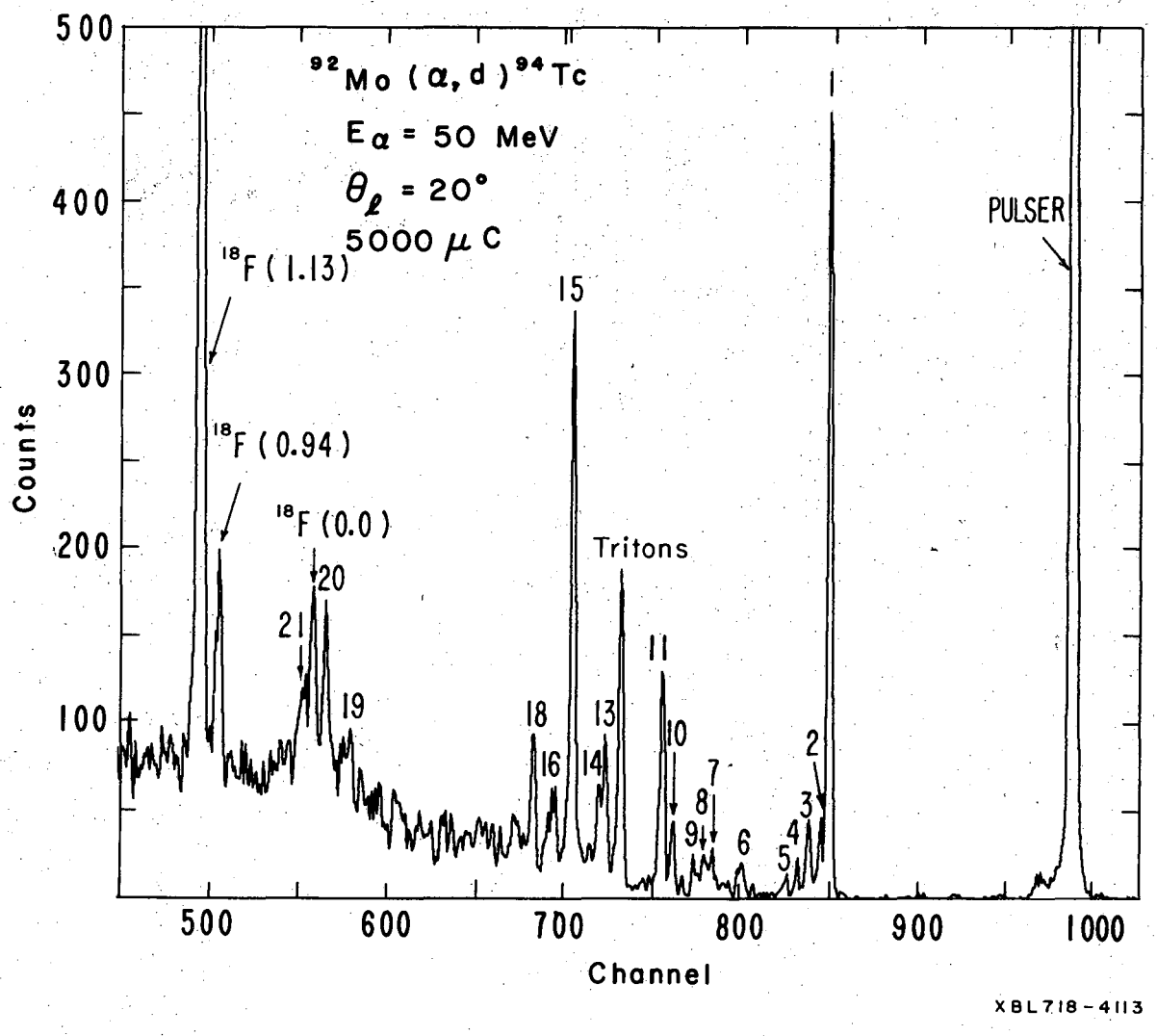
^{92}Mo (α, d) ^{94}Tc
E_α = 50 MeV
θ_ℓ = 20°
5000 μC
^{18}F (1.13)
^{18}F (0.94)
^{18}F (0.0)
Tritons
PULSER
Counts
Channel
XBL718-4113

Fig. 9

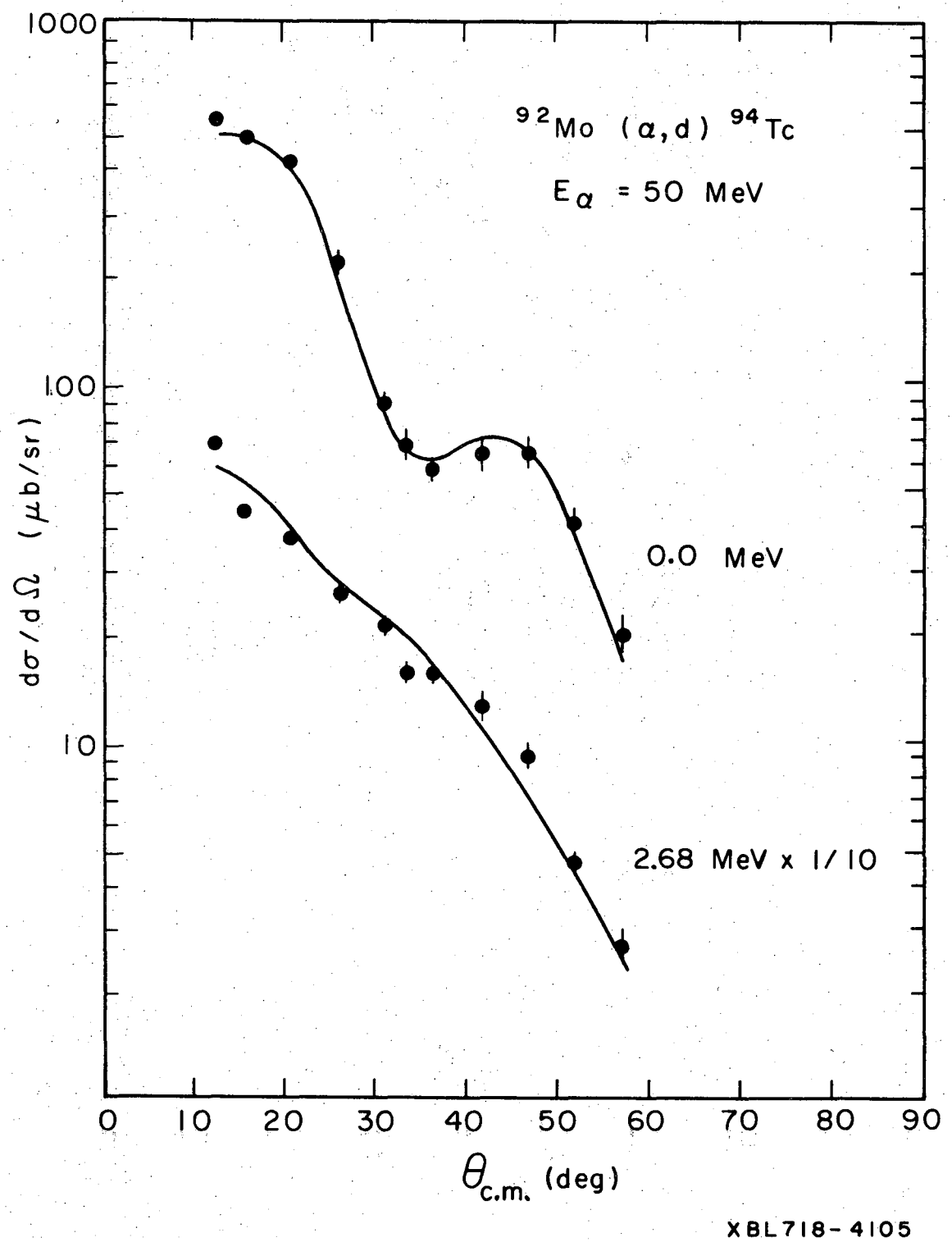
1000
100
10
^{92}Mo (α,d) ^{94}Tc
E_α = 50 MeV
0.0 MeV
2.68 MeV x 1/10
dσ/dΩ (μb/sr)
0
10
20
30
40
50
60
70
80
90
$\theta_{c.m.}$ (deg)
XBL718-4105

Fig. 10

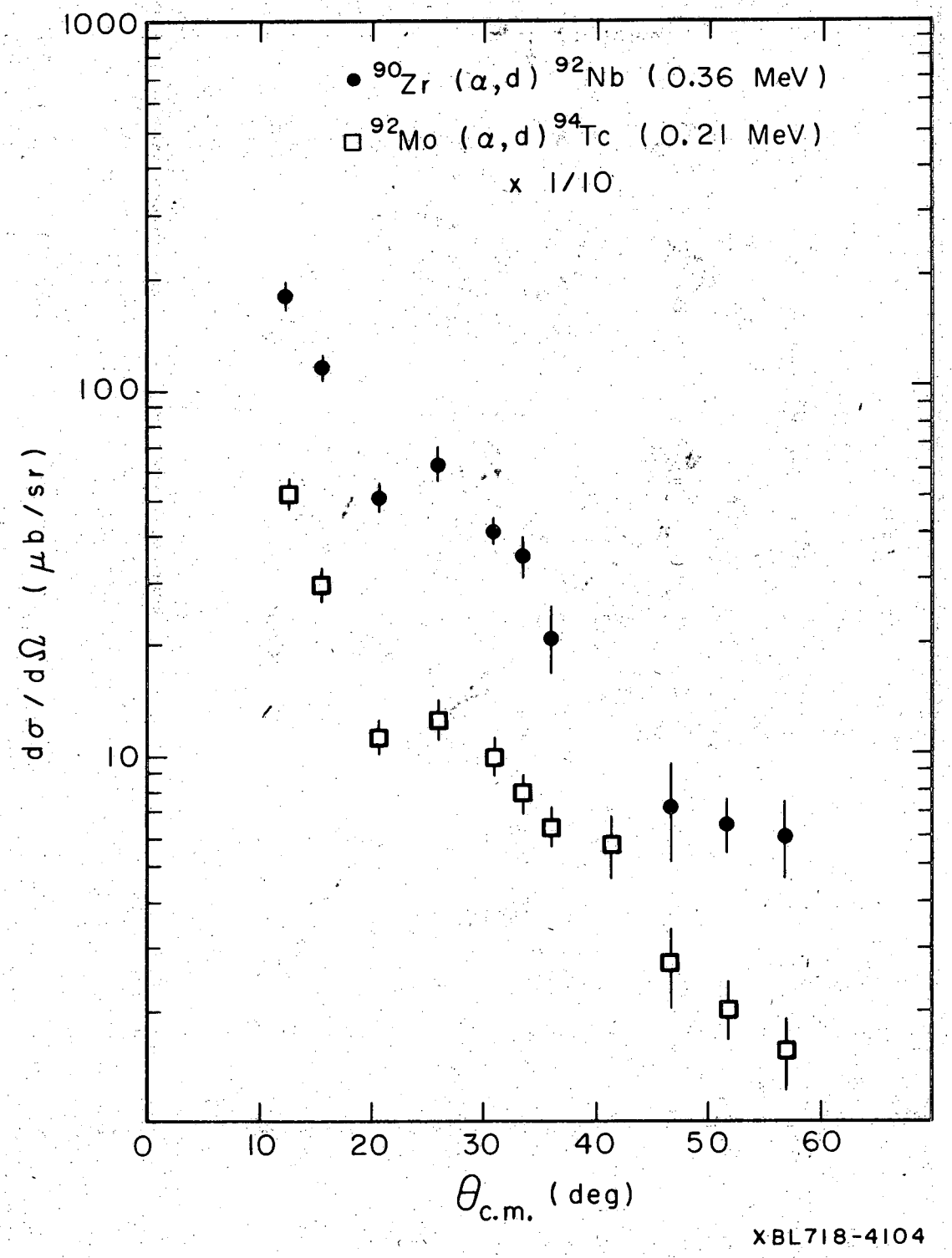
1000
100
10
0
10
20
30
40
50
60
● ^{90}Zr (α,d) ^{92}Nb (0.36 MeV)
□ ^{92}Mo (α,d) ^{94}Tc (0.21 MeV)
x 1/10
dσ/dΩ (μb/sr)
θc.m. (deg)
XBL718-4104

Fig. 11

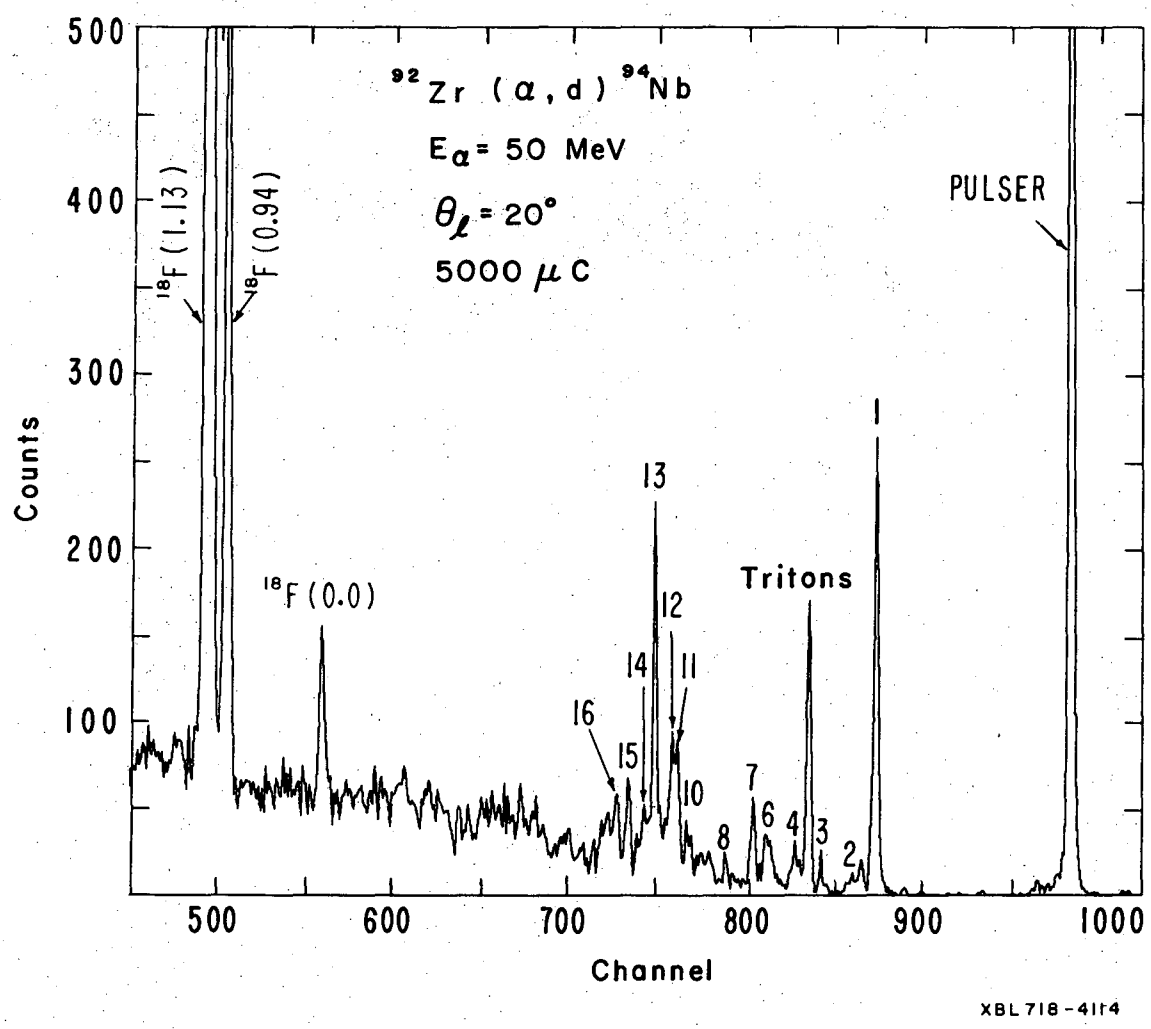
^{92}Zr (α, d) ^{94}Nb
E_α = 50 MeV
θ_ℓ = 20°
5000 μC
^{18}F (1.13)
^{18}F (0.94)
^{18}F (0.0)
PULSER
Tritons
1
2
3
4
6
7
8
10
11
12
13
14
15
16
Counts
Channel
500
400
300
200
100
500
600
700
800
900
1000
XBL 718-4114

Fig. 12

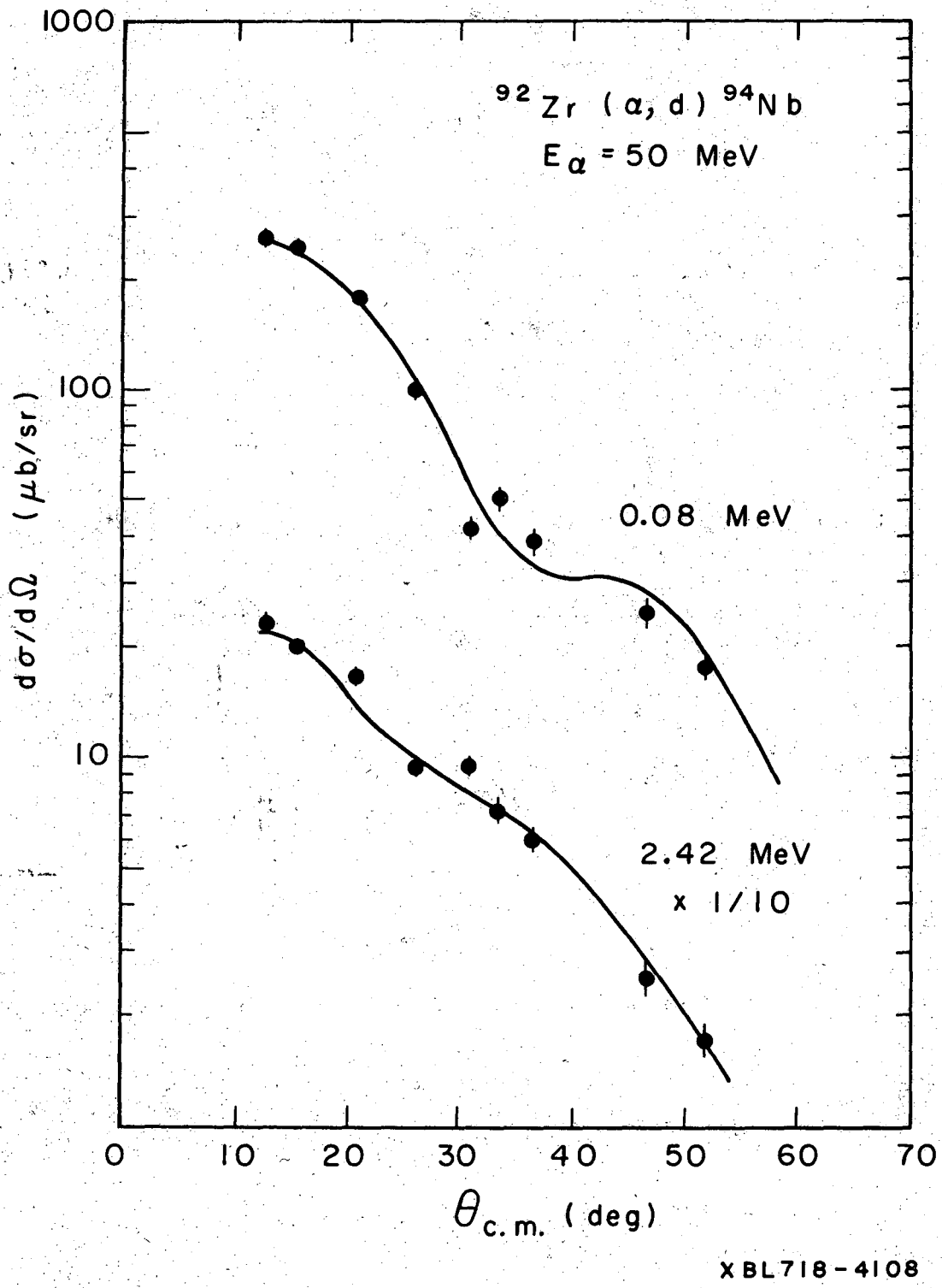
^{92}Zr (α, d) ^{94}Nb
E_α = 50 MeV
0.08 MeV
2.42 MeV
x 1/10
1000
100
10
dσ/dΩ (μb/sr)
0
10
20
30
40
50
60
70
$\theta_{c.m.}$ (deg)
XBL718-4108

Fig. 13

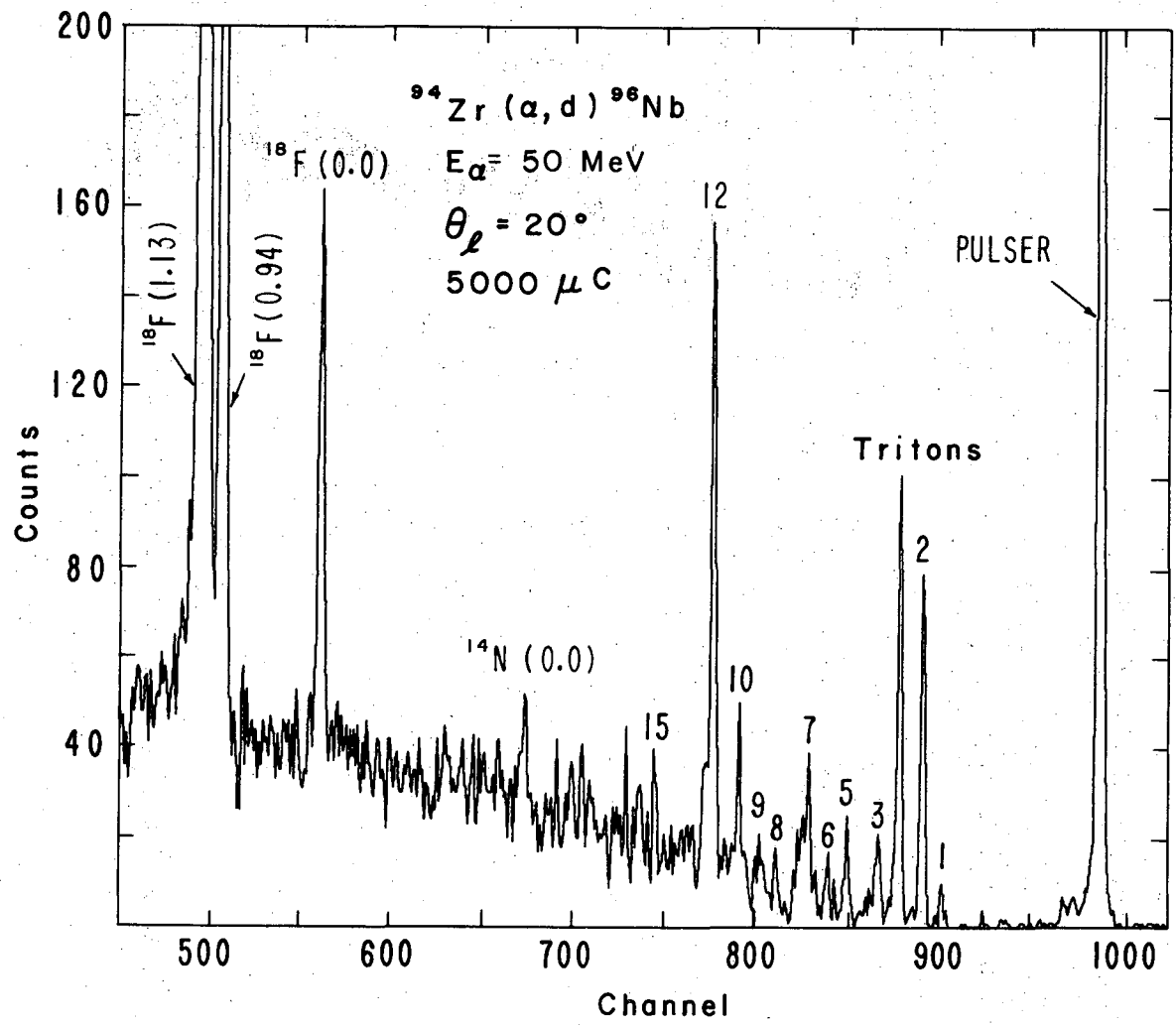

XBL 718 - 4115

Fig. 14

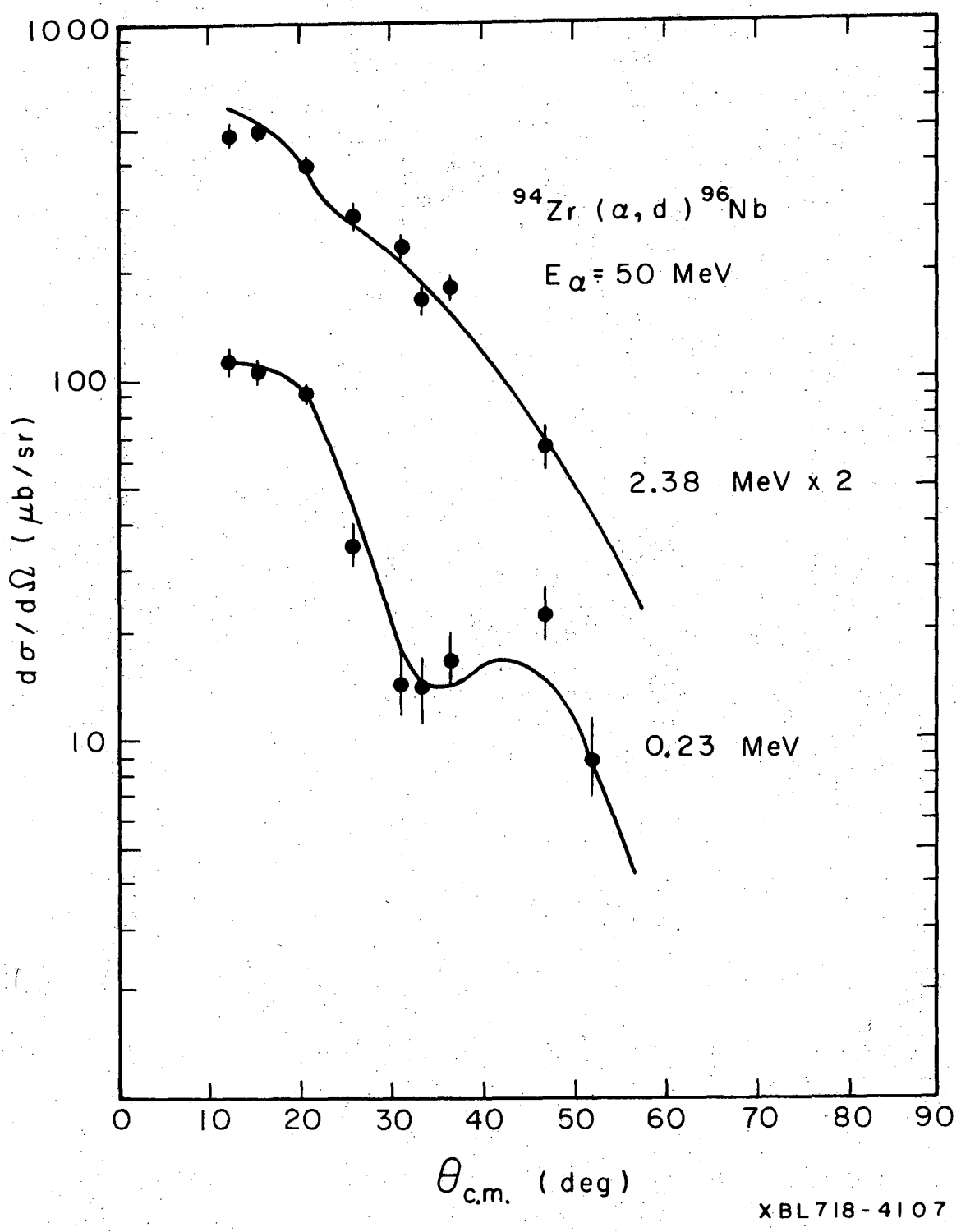
1000
100
10
$d\sigma/d\Omega$ (μb/sr)
^{94}Zr (α, d) ^{96}Nb
E_α = 50 MeV
2.38 MeV x 2
0.23 MeV
0
10
20
30
40
50
60
70
80
90
$\theta_{c.m.}$ (deg)
XBL718-4107

Fig. 15

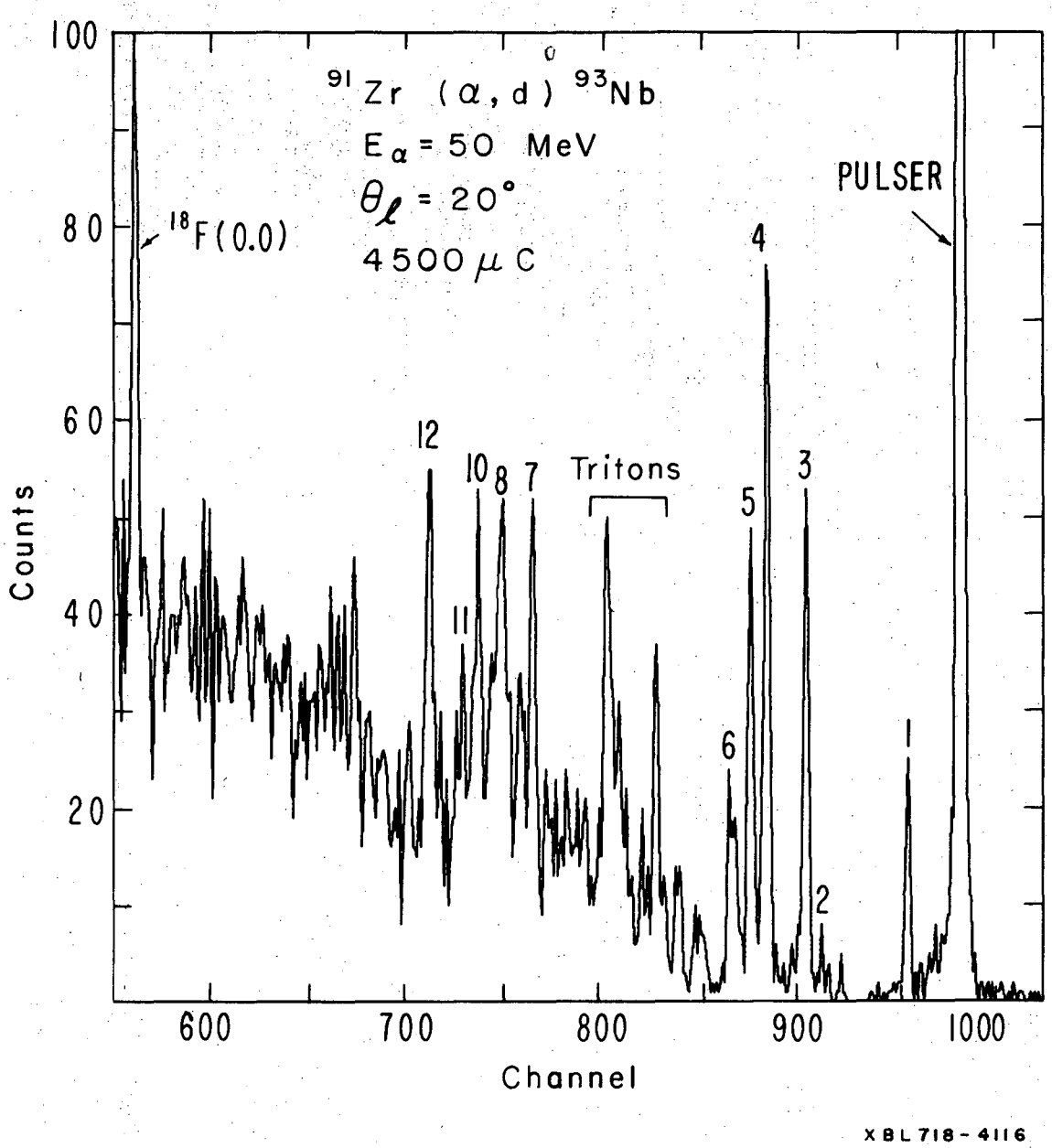

XBL 718-4116

Fig. 16

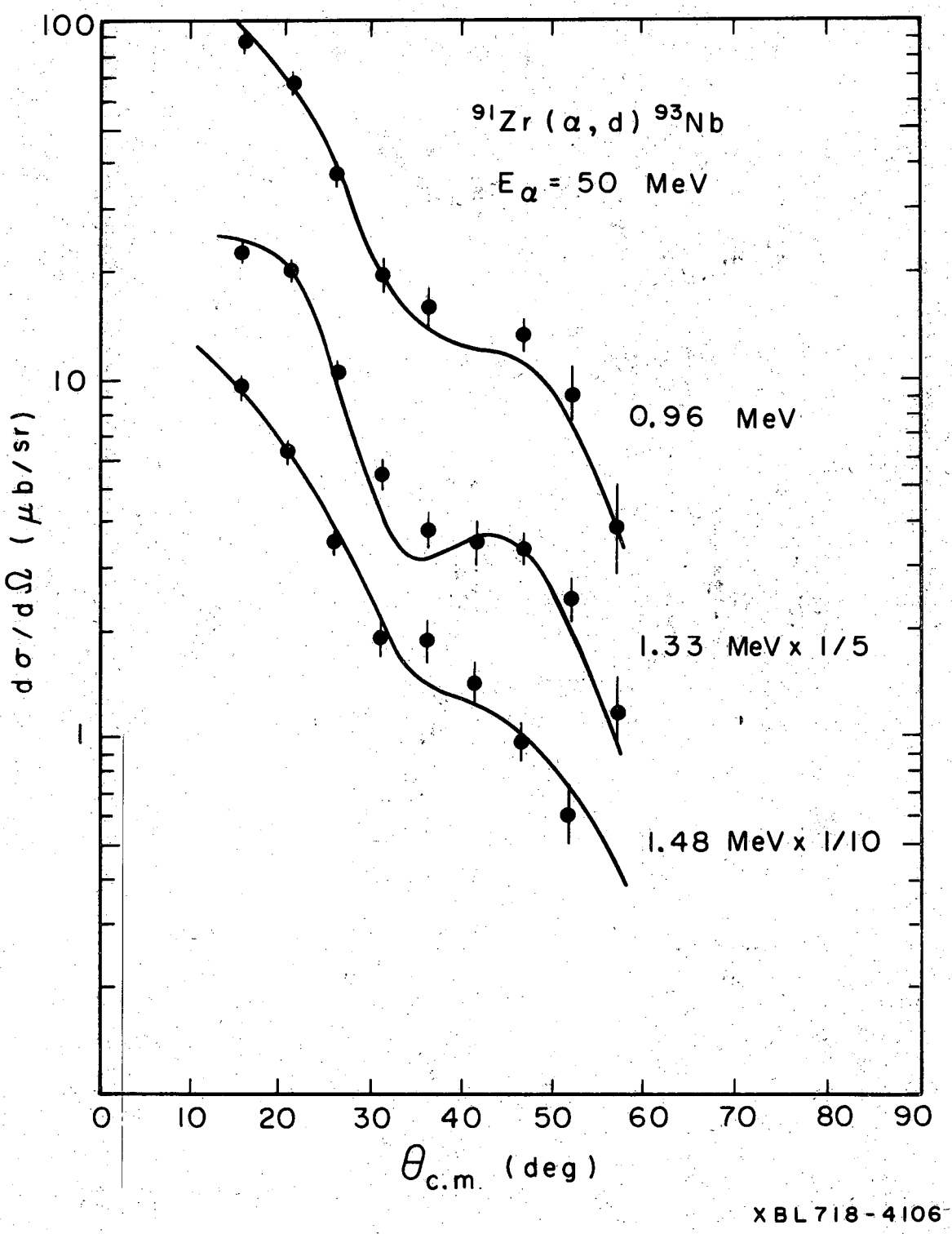
$^{91}Zr(\alpha, d)^{93}Nb$
$E_\alpha = 50$ MeV
0.96 MeV
1.33 MeV x 1/5
1.48 MeV x 1/10
100
10
1
$d\sigma/d\Omega$ (μb/sr)
0
10
20
30
40
50
60
70
80
90
$\theta_{c.m.}$ (deg)
XBL718-4106

Fig. 17

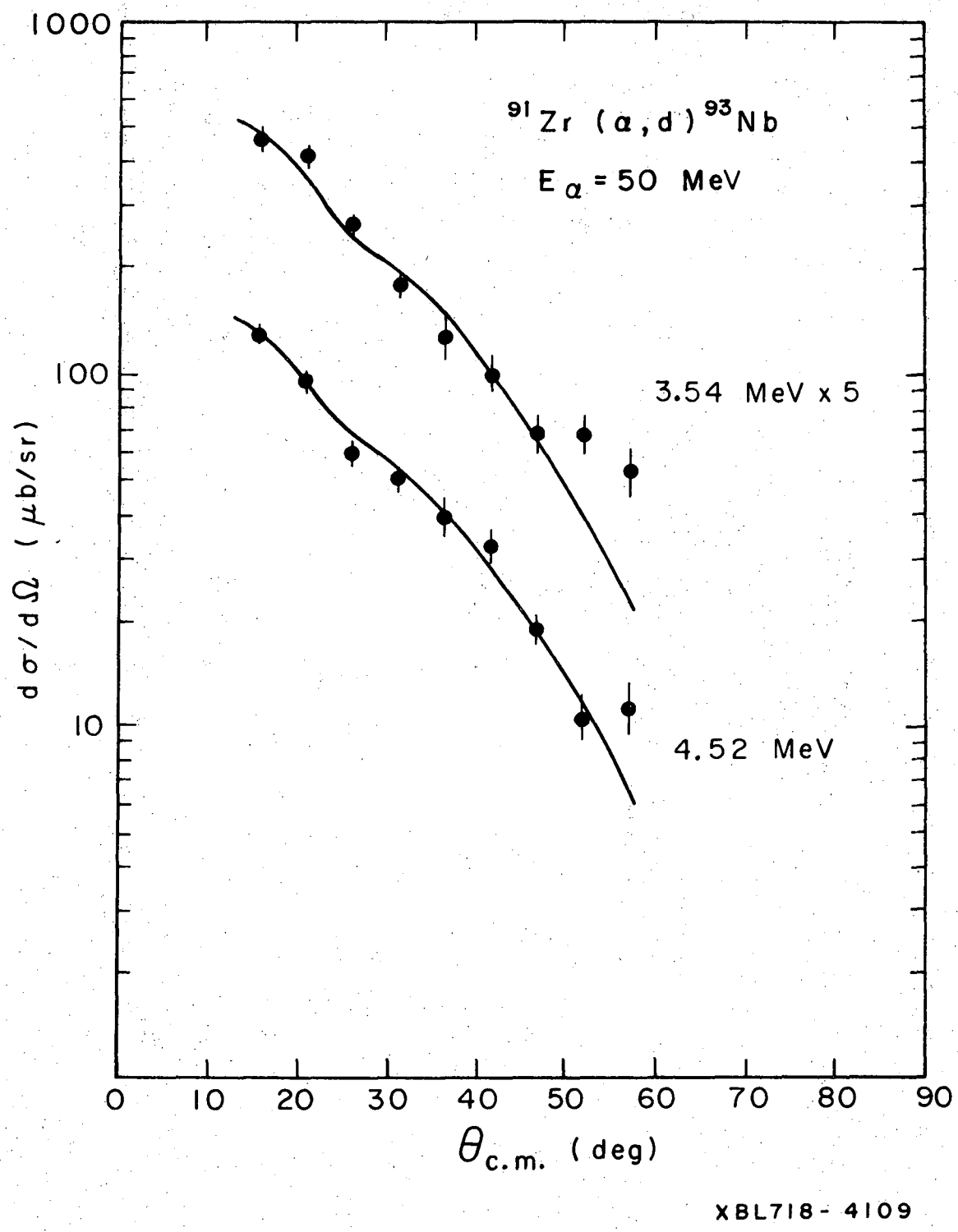
^{91}Zr (α, d) ^{93}Nb
E_α = 50 MeV
3.54 MeV x 5
4.52 MeV
1000
100
10
dσ/dΩ (μb/sr)
0
10
20
30
40
50
60
70
80
90
$\theta_{c.m.}$ (deg)
XBL718-4109

Fig. 18

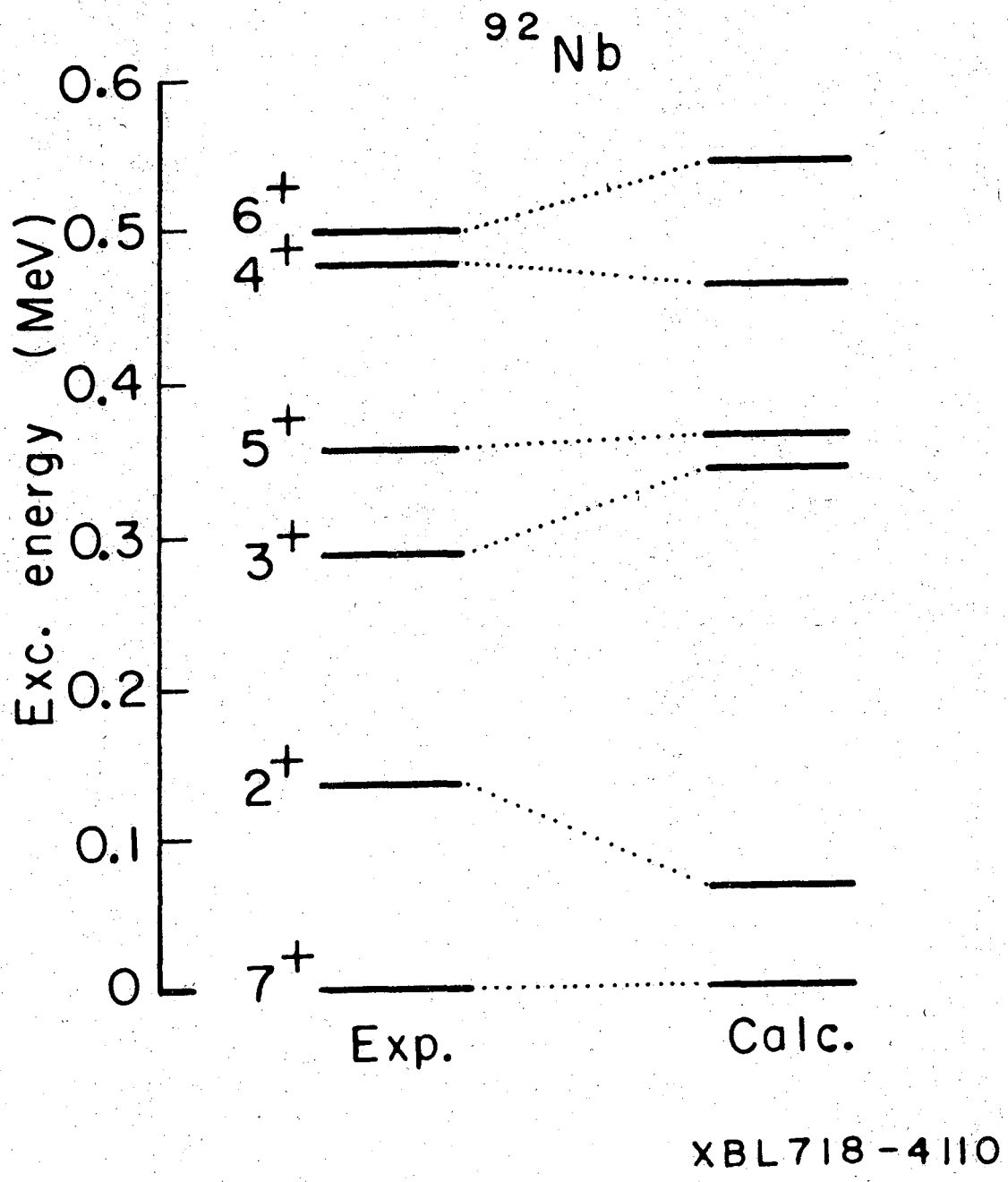
92Nb
0.6
0.5
0.4
0.3
0.2
0.1
0
Exc. energy (MeV)
6+
4+
5+
3+
2+
7+
Exp.
Calc.
XBL718-4110

Fig. 19

LEGAL NOTICE

This report was prepared as an account of work sponsored by the United States Government. Neither the United States nor the United States Atomic Energy Commission, nor any of their employees, nor any of their contractors, subcontractors, or their employees, makes any warranty, express or implied, or assumes any legal liability or responsibility for the accuracy, completeness or usefulness of any information, apparatus, product or process disclosed, or represents that its use would not infringe privately owned rights.

TECHNICAL INFORMATION DIVISION
LAWRENCE RADIATION LABORATORY
UNIVERSITY OF CALIFORNIA
BERKELEY, CALIFORNIA 94720